REPORT No. 697

INVESTIGATIONS ON THE INCOMPLETELY DEVELOPED PLANE DIAGONAL-TENSION FIELD

By Paul Kuhn

SUMMARY

Actual diagonal-tension beams work in an intermediate stage between pure shear and pure diagonal tension; the theory developed by Wagner for diagonal tension is therefore not directly applicable. This paper presents the results of investigations on the incompletely developed diagonal-tension field.

The first part of the paper briefly reviews the most essential items of the theory of pure diagonal tension as well as previous attempts to formulate a theory of incomplete diagonal tension. A simple semiempirical theory of incomplete diagonal tension that includes the cases of pure shear and of pure diagonal tension as limiting cases is then presented.

The second part of the paper describes strain measurements made by the N. A. C. A. to obtain the necessary coefficients for the proposed theory. Some measurements of buckling deflections were also made by the N. A. C. A. Strain measurements and deflection measurements made elsewhere are evaluated in the light of the proposed theory.

The third part of the paper discusses the stress analysis of diagonal-tension beams by means of the proposed theory.

An attempt has been made to utilize all available material so that the current state of knowledge on the stress analysis of diagonal-tension beams might be presented in a form useful to the stress analyst.

INTRODUCTION

The basic concept of diagonal-tension beams was introduced into aeronautical literature by Wagner in reference 1, which presents a very complete theory. The principles of this theory, insofar as they interest the practical designer, are summarized in reference 2. Brief reviews of the basic principles of the theory are also given in a number of other articles and textbooks, such as references 3 and 4.

Experience has shown that the theory of diagonal tension as presented in references 1 to 4 is, in many cases, entirely too conservative. The principal reason for the discrepancy between theory and experimental data is evidently the fact that the sheet continues to carry shear, that is, diagonal compression, after buckling so that the state of pure diagonal tension is only a theoretical limiting case which is asymptotically approached but never reached in an actual structure. Wagner himself published, in reference 5, the results of a series of tests designed to give empirical data for incomplete diagonal-tension fields, but doubts have been voiced about the applicability of the results to diagonal-tension beams of practical proportions. The N. A. C. A. therefore conducted an investigation of diagonal-tension beams, the results of which form the subject of this paper.

The paper is divided into three parts. The first part deals with the theory. Wagner's theory of the pure diagonal-tension field is briefly reviewed, as are previous attempts to develop a theory for the incomplete diagonal-tension field. A simple semiempirical theory for the incomplete diagonal-tension field is then presented; this theory includes as limiting cases the cases of pure shear and of pure diagonal tension. The buckling under shear stresses of unstiffened sheet and of stiffened sheet is discussed.

The second part of the paper deals with the experimental results. Strain measurements made by the N. A. C. A. are described; these tests were used to establish the coefficients for the proposed semiempirical theory. The results are well confirmed by measurements made by the Douglas Aircraft Co. on a large beam; thanks are due the Douglas Co. for their courtesy in permitting the publication of these results. On three of the N. A. C. A. test set-ups, the buckling deflections of the uprights were measured; these tests as well as other tests on buckling are discussed. The N. A. C. A. tests were performed in the spring and summer of 1939 by Patrick T. Chiarito of the Laboratory staff.

The third part of the paper shows how the results of this investigation are applied to stress analysis.

The three parts of this paper are largely independent of each other, but it is recommended that part I be read before using part III.

I. THEORIES OF DIAGONAL-TENSION ACTION AND AUXILIARY THEORIES

THEORY OF THE PURE DIAGONAL-TENSION FIELD

The theory of beams with webs working in pure diagonal tension was presented by Wagner in reference 1. It assumes that the sheet constituting the web of the beam has no bending stiffness. Under the action of the shear stresses, the web will then form a large number of narrow and shallow folds inclined at an angle α to the flanges; the stress in the sheet is pure tension in the direction of the folds. The theory given in reference 1 is so comprehensive that no additional contributions of

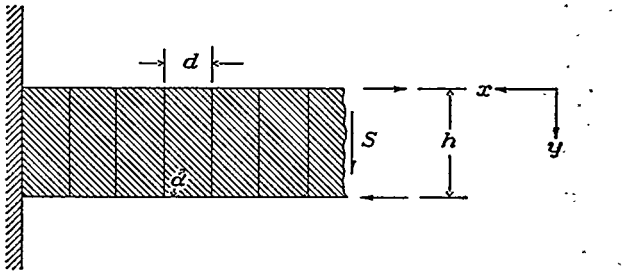

FIGURE 1.—Diagonal-tension beam.

great importance have been made since it was published. Mention might be made of the study given in reference 6 dealing with beams having sharply inclined flanges.

The essential principles and results of the theory have been given in several places, for instance, in references 2, 3, and 4, and are sufficiently well known to aeronautical engineers to obviate very detailed discussion here. It will suffice to recall that the basic case is that shown in figure 1. If the flanges and the uprights are heavy, the angle α is 45°; the compressive force on each upright is then

$$V=S\frac{d}{h} \tag{1}$$

Each flange is acted upon by the primary beam force $F=M/h$ and by a compressive force

$$H=\frac{S}{2} \tag{2}$$

that balances the horizontal component of the diagonal tension in the sheet. The tensile stress in the web is

$$\sigma=\frac{2\tau}{C_2}=2\frac{S}{htC_2} \tag{3}$$

where t is the thickness of the sheet and τ is the nominal shear stress, while C_2 is a stress-concentration factor that depends on the flexibility of the flanges (references 1 and 2). The factor C_2 was given by Wagner as a function of a flexibility parameter designated ωd and defined by

$$\omega d=0.89d\sqrt[4]{\frac{t}{(I_T+I_C)h}} \tag{4}$$

where I_T and I_C are the moments of inertia of the tension flange and the compression flange, respectively (references 1 and 2).

The secondary bending moments in the flanges caused by the vertical component of the diagonal tension are given by

$$M=k_M C_1 S d^2/h \tag{5}$$

where $k_M=1/12$ over the uprights and $k_M=1/24$ midway between the uprights. The factor C_1 again depends on the flexibility parameter ωd (references 1 and 2).

For convenience, the graph showing C_1 and C_2 is reproduced here from reference 1 as figure 2.

If each flange is inclined at a moderate angle $\delta/2$ to the horizontal axis of the beam, the shear S in equations (1) to (5) is the web shear given by

$$S_W=S_E-\frac{M}{h}\tan\delta \tag{6}$$

where S_E is the external, or applied, shear.

Beams that differ materially from the basic case, for instance, beams with inclined uprights or sharply inclined flanges or beams with axial load, will not be discussed in this paper.

PREVIOUS THEORIES OF INCOMPLETE DIAGONAL-TENSION FIELD

Practical experience has shown that the theory of pure diagonal tension is, in many cases, entirely too conservative. The principal reason for the disagreement between theory and experiment will be found by considering the stresses due to shear acting in the web

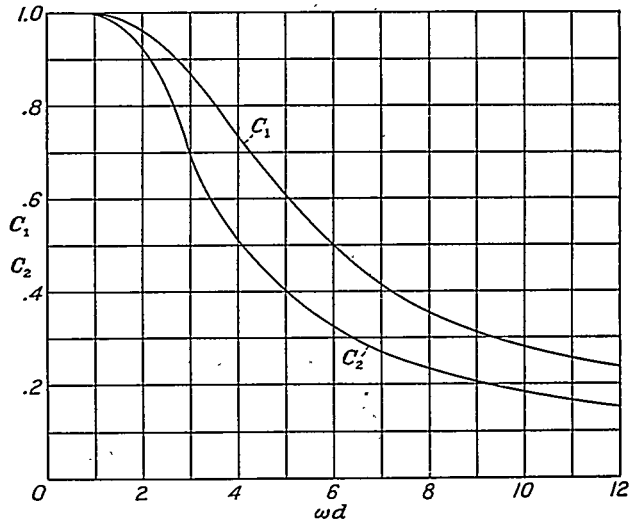

FIGURE 2.—Theoretical stress factors for pure diagonal tension (from reference 1).

sheet after buckling; the stresses in the web due to beam action are neglected in this discussion.

The state of pure shear that exists up to the buckling point in the web is equivalent to tensile and compressive stresses of equal magnitude acting at angles of 45° to the horizontal and the vertical axes. In the pure diagonal-tension field, the compressive stress is zero and the tensile stress is twice as much as it would be in the corresponding state of pure shear. As the shear force on a beam web increases beyond the buckling point, however, the compressive stress corresponding to the shear does not vanish suddenly and completely.

Some compressive stress continues to exist, and this diagonal compression combines with part of the diagonal tension into a shear stress. As the shear force increases to higher and higher values, the relative importance of the compressive stress decreases and the condition of pure diagonal tension is approached more and more closely but is never quite reached in an actual beam. The finite strength of the material will permit a failure before the diagonal-tension field is fully developed; in other words, practical design has to deal with webs constituting an incompletely developed diagonal-tension field somewhere between the limiting stages of pure shear and pure diagonal tension.

A number of authors have adopted an assumption sometimes used in the analysis of trusses with double diagonals, namely, that the compressive stress remains constant after buckling and equal to the stress at buckling. Under this assumption, only the excess stress over the buckling shear stress is converted into diagonal tension, while a shear stress equal in magnitude to the buckling stress is carried by the sheet as true shear. This assumption can be written

$$\tau_{DT}=\tau-\tau_{cr}=\tau(1-\tau_{cr}/\tau) \tag{7}$$

where τ is the purely nominal applied shear stress S/ht, τ_{DT} is the part of the applied shear stress that is carried as diagonal tension, and τ_{cr} is the critical stress that continues to exist as a true shear stress. The second form of writing the expression indicates that the diagonal tension is a function of the ratio τ_{cr}/τ, which is the inverse of the loading ratio τ/τ_{cr}, that is, the ratio of the applied stress to the buckling stress or of the applied load to the buckling load.

Wagner himself proposed (reference 7) to apply the assumption expressed by equation (7) to the analysis of curved diagonal-tension fields. In such fields, the loading ratio τ/τ_{cr} at the design load probably never exceeds 10 and is generally below 5 because the folds become objectionably deep soon after buckling occurs and permanent set and failure soon follow.

In plane diagonal-tension fields, the loading ratio is, as a rule, much higher than in curved fields and equation (7) was experimentally found to be inadequate to deal with such cases. Realizing this weakness of the theory, Wagner conducted experiments (reference 5) that were intended to give empirical relations for the stresses in incomplete diagonal-tension fields. Questions have been raised, however, about the direct applicability of the test results to practical design.

Schapitz (references 8 and 9) developed a theory of the incomplete diagonal-tension field, including at the same time the effect of superposed normal stresses on the panel. He began with an assumption on the stress distribution within the panel, leaving one basic parameter (two for curved panels) free to be adjusted so that the results would fit experiments. Like all other authors preceding him, he assumed the diagonal compression to be constant after buckling. Attempts to correlate this theory with the N. A. C. A. tests have been unsuccessful.

407300°—41——26

PROPOSED NEW THEORY OF INCOMPLETE DIAGONAL-TENSION FIELD

Test observations have shown that the behavior of a shear web working in partial diagonal tension is often quite irregular and is apparently influenced by a number of factors which cannot be evaluated. This observation is, of course, merely a repetition of similar experiences in the study of built-up structures of thin sheet metal, but it again emphasizes the fact that too much accuracy should not be expected from a "rigorous" and perhaps mathematically very elaborate theory if the physical action of such complicated structures depends on entirely too many unknown and uncontrollable factors. In view of the fact that the ultimate aim of any engineering theory of stresses is application to practical design work, it seems rational under such circumstances to develop a theory with an eye toward ease of application.

A modification of the theory given in reference 10 for curved diagonal-tension fields was found to describe the experimental facts with an accuracy compatible with the scatter of the test points. The basic assumption of this theory is that the total shear force in the web can be divided into a shear force carried by shear in the sheet and a shear force carried by diagonal tension; this assumption may be written as

$$S=S_S+S_{DT}$$

or

$$S_{DT}=kS \text{ and } S_S=(1-k)S \tag{8}$$

where k is the fraction of the total shear that is carried as diagonal tension.

The diagonal-tension fraction k is assumed to be given by the expression

$$k=(1-\tau_{cr}/\tau)^n \tag{9}$$

The form of this expression was suggested by formula (7). According to Wagner (reference 5), the degree of development of the diagonal tension is a function of σ_U/τ, where σ_U is the compressive stress in the upright. Experimental values of n derived from the N. A. C. A. tests to be described in part II were therefore plotted against σ_U/τ; the relation between n and σ_U/τ could be expressed by

$$n=1+5\sigma_U/\tau \tag{10}$$

For beams with very heavy uprights ($\sigma_U \to 0$) the assumption expressed by equations (8), (9), and (10) reduces to that given by equation (7); that is, the true shear in the sheet remains constant after the buckling load is passed. For finite values of σ_U, however, the true shear continues to increase according to equations (8), (9), and (10) after the buckling load has been passed. This distinction is the main difference between the proposed new theory and the existing theories.

It is assumed, at variance with the assumptions of reference 10, that a certain effective width of sheet aids the uprights in carrying the compression stresses due to the vertical component of diagonal tension; similarly, a certain effective width of sheet is assumed to aid the flanges in carrying the compression stresses due to the horizontal component of diagonal tension. In each case, the effective width is assumed to be proportional to the amount of true shear stress in the sheet; the effective cross-sectional area of the upright is therefore

$$A_{U_e}=A_U+(1-k)td \tag{11}$$

where A_U is the area of the upright proper; the effective area of each flange is

$$A_{F_e}=A_F+\tfrac{1}{2}(1-k)ht \tag{12}$$

The manner of measuring the areas and the distances of the preceding equations is indicated in figure 3.

Before the effects of the diagonal tension can be computed, the angle α of the diagonal tension must be

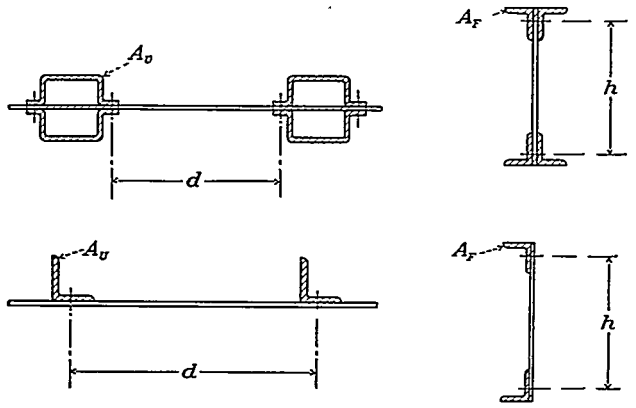

FIGURE 3.—Conventions for measuring distances and areas.

found. It should be borne in mind that the direction of the folds is of no interest; only the direction of diagonal tension is of interest. In the pure diagonal-tension field the direction of the diagonal tension coincides with the direction of the folds. In the incomplete diagonal-tension field, however, there is no such simple relation, quite aside from the fact that the shape of the sheet shortly after passing the buckling load can hardly be described as a series of straight and parallel folds, as a glance at the contour map of the deflection surface will show (references 4 and 11). A general qualitative consideration of the theory of buckling under shear stresses (references 4 and 11), of pure diagonal-tension theory (reference 1), and of all available test results led to the conclusion that it should be sufficiently accurate to assume the angle of diagonal tension α to be 45° when dealing with beams reasonably close to the basic case of figure 1. If the average actual angle differs from 45° (according to Wagner, it is about 40° or 42° for pure diagonal tension), the difference will be automatically taken care of by the experimental determination of the exponent n in equation (9). The importance of variations of α due to change of design proportions within probable limits will be overshadowed by scatter due to unknown and uncontrollable causes.

With the assumptions previously enumerated, the formula for the stress in an upright is obtained by combining equations (1), (8), and (11) as

$$\sigma_U=\frac{kSd}{hA_{U_e}}=\frac{kSd}{h[A_U+(1-k)dt]}=\frac{k\tau td}{A_U+(1-k)dt} \tag{13}$$

The formula for the compression stress in the flange caused by the diagonal tension is obtained by combining equations (2), (8), and (12) as

$$\sigma_F=\frac{kS}{2A_{F_e}}=\frac{kS}{2A_F+(1-k)ht} \tag{14}$$

Formula (13) must be solved by trial and error because k is a function of σ_U. A value of σ_U is assumed; n is calculated by formula (10); k, by equation (9); and, finally, σ_U, by equation (13). If this value does not agree with the assumed value, the process is repeated with an improved value. Three repetitions of the computation are usually sufficient to obtain a precision of about 1 percent or better, but the process is somewhat tedious because it involves fractional powers.

Figure 4 is a chart that eliminates the necessity of this calculation in most practical cases. In stress-analysis work, the shear stress τ and the ratios τ/τ_{cr} and A_U/td will be given and σ_U/τ can be found from the chart, so that σ_U is determined. The diagonal-tension fraction k can then be calculated from

$$k=\frac{\sigma_U(1+A_U/td)}{\tau(1+\sigma_U/\tau)} \tag{15}$$

or it can be found from figure 4 by inspection and σ_F can be found by using equation (14).

The secondary bending moments in the flanges will be calculated by using equation (5) after substituting S_{DT} for S. The values to be used for k_M will be discussed in part II; the experimental evidence shows the theoretical values $\frac{1}{12}$ and $\frac{1}{24}$ to be unsatisfactory.

The design chart of figure 4 corresponds to the design chart given by Lahde and Wagner in reference 5. Comparison of the two design charts shows that the chart of figure 4 is considerably less optimistic than the one of reference 5; in order to keep the stresses in the uprights of a given beam down to a given allowable value, figure 4 demands a larger cross-sectional area of the uprights than does the chart of reference 5.

BUCKLING OF FLAT SHEET SUBJECTED TO SHEAR STRESSES

The exact solution for the critical shear stress of an infinitely long plate given in reference 11 includes the case of the plate with clamped edges as well as the case of the plate with supported edges. Approximate solutions for plates of finite length with supported edges are given by Timoshenko (references 4 and 12). A few approximate values for plates of finite length with clamped edges are given in reference 13.

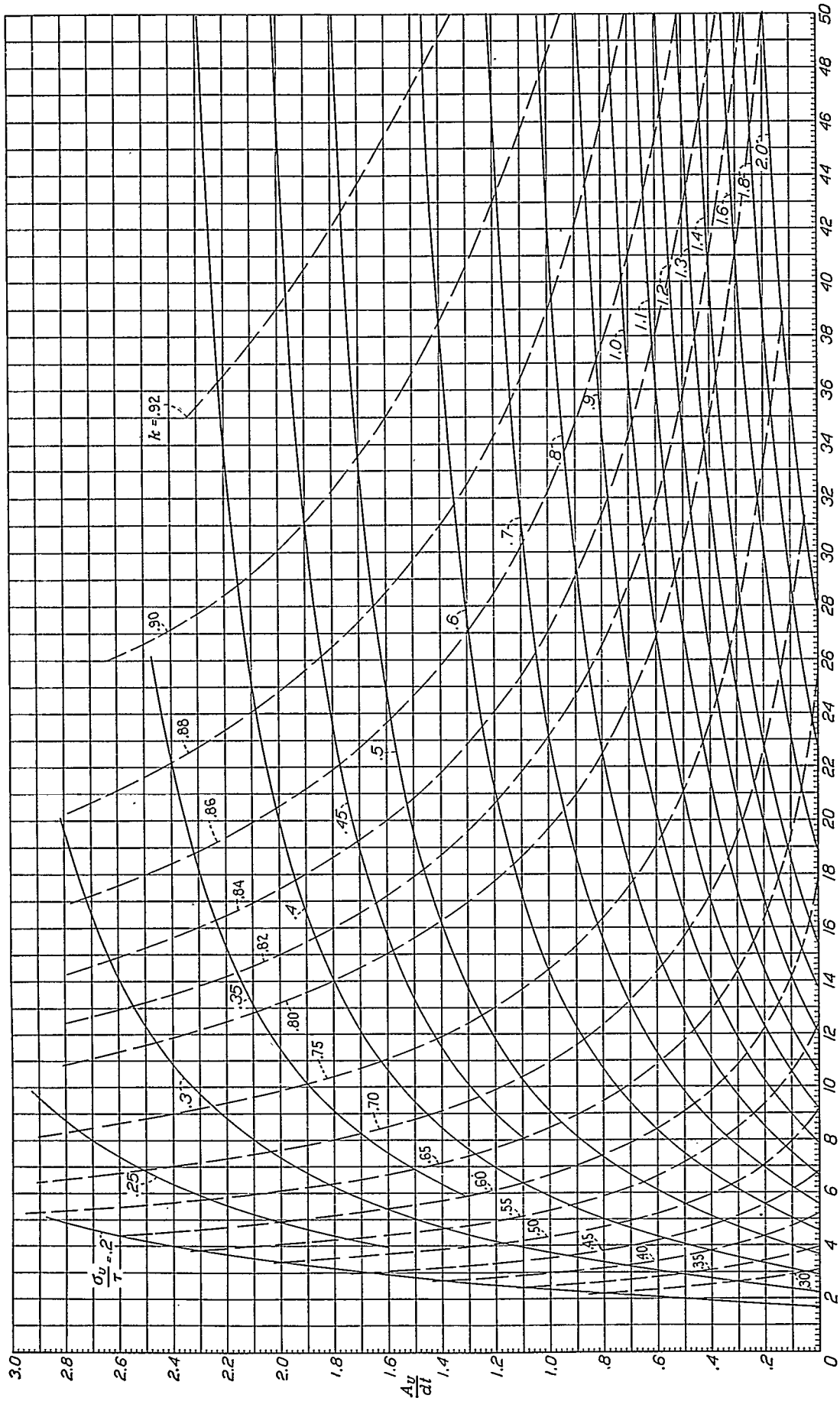

FIGURE 4.—Design chart for stresses in incomplete diagonal-tension fields.

The critical stress can be expressed by the general equation

$$\tau_{cr}=KE(t/b)^2 \tag{16}$$

The values of K are given in figure 5, which is based on average values from all the sources just named.

No solutions appear to have been published for plates with some edges clamped and some edges supported. Approximate values for K may be obtained for such cases by interpolating between the two curves

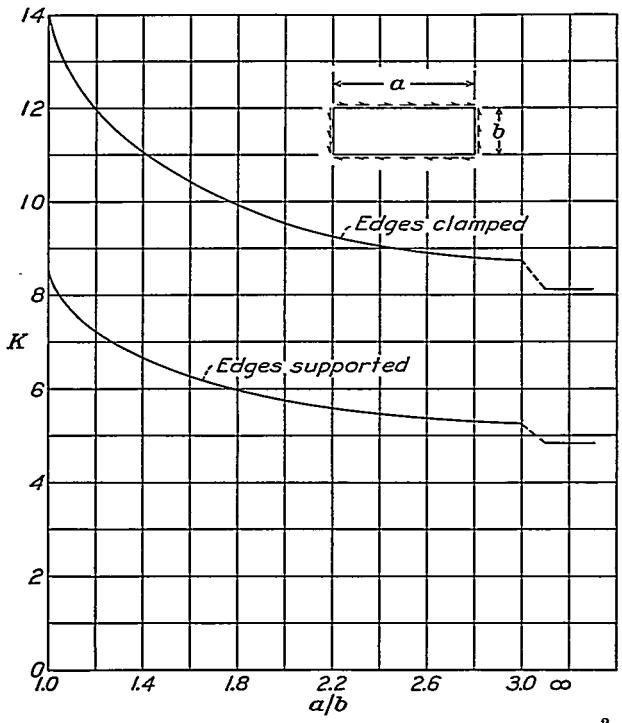

FIGURE 5.—Critical shear stress for isotropic plates. $\tau_{cr}=KE(t/b)^2$.

of figure 5 with the ratio of the length of the clamped edges to the total length of all four edges of the plate.

BUCKLING OF ORTHOTROPIC PLATES SUBJECTED TO SHEAR STRESSES

An anisotropic plate is a plate that has different elastic properties in different directions. It can be represented by a plate with two systems of stiffeners attached to it. In the particular case in which the two sets of stiffeners are at right angles to each other, the plate is called orthogonally anisotropic or, briefly, orthotropic. If the uprights of a plate girder are arranged at right angles to the axis of the beam, the web with the uprights constitutes an orthotropic plate; in this case the second stiffener system at right angles to the main system is merged with the plate; that is, the plate itself constitutes the second stiffener system.

On reaching a certain critical shear load, an orthotropic plate will form buckles similar to the shear buckles formed by an isotropic plate. This buckling involves the sheet and a large number of stiffeners at the same time and is therefore sometimes referred to as "general elastic instability" in order to differentiate it from "local instability," which involves only the sheet panels between stiffeners. The critical shear force at which an infinitely long plate with supported edges begins to buckle is given by references 14 to 17 as

$$S_{cr}=17.5E\frac{1}{h}\sqrt[4]{\frac{I^3t^3}{d^3}} \tag{17}$$

where I is the moment of inertia of one upright including the sheet and d is the distance between the center lines of uprights. If the edges are clamped, the factor 27.8 is substituted for 17.5. It should be noted that clamping of the edges involves two requirements: The sheet and the uprights must be clamped to the beam flanges, and the beam flanges must be prevented from twisting about their longitudinal axes. In actual structures, the flanges will probably be much closer to the supported condition than to the clamped condition.

The half-wave length of the buckles is given by

$$\lambda=0.55h\sqrt[4]{\frac{dt^3}{I}} \tag{18}$$

for a plate with supported edges; for a plate with clamped edges, the coefficient 0.55 is changed to 0.37.

The theory is strictly valid only if the stiffener spacing d is infinitely close. For practical purposes, the influence of finite stiffener spacing may be expected to be negligible if $d<\lambda/3$. The limit of applicability is reached theoretically when d is about equal to λ, but good agreement has been found experimentally in a few cases when this limit was slightly exceeded (reference 16).

Equations (17) and (18) are obtained from the theory of references 14 to 17 on the simplifying assumption that the horizontal bending stiffness per running inch $I_h=t^3/12$ is negligible compared with the vertical bending stiffness per running inch $I_v=I/d$, or that the ratio $12I/dt^3$ is large. In the limiting case of a sheet without stiffeners, when this ratio equals unity, equation (17) gives a critical stress about 44 percent too low.

It should be remembered that the theory of anisotropic buckling strictly applies only to a plate girder in which the web has not buckled between uprights into a diagonal-tension field. As long as the loading ratio is not too high, however, the theory should apply reasonably well to diagonal-tension beams.

BUCKLING OF UPRIGHTS IN DIAGONAL-TENSION FIELDS

The uprights in diagonal-tension fields act as columns and are therefore subjected to the same general types of failure that occur in free columns, namely, primary column failure by general buckling or bending, primary column failure by twisting, and secondary failure by local buckling or crippling (reference 18). The presence of the web, however, may modify the details of the failures and may materially change the stresses at which the failures occur, assuming that the uprights are riveted to the web as is standard practice.

Primary column failure by buckling out of the plane of the web is the most obvious possibility of failure and was thoroughly investigated by Wagner in reference 1 for the pure diagonal-tension field. The web under diagonal tension acts as an elastic foundation for the uprights and stabilizes them against buckling. Curves giving the ratios of the theoretical buckling load V_T of the uprights to their Euler loads P_E were shown in reference 1 and are reproduced for convenience in figure 6.

The load V_T applies directly only when the uprights are very long. In general, it will be necessary to com-

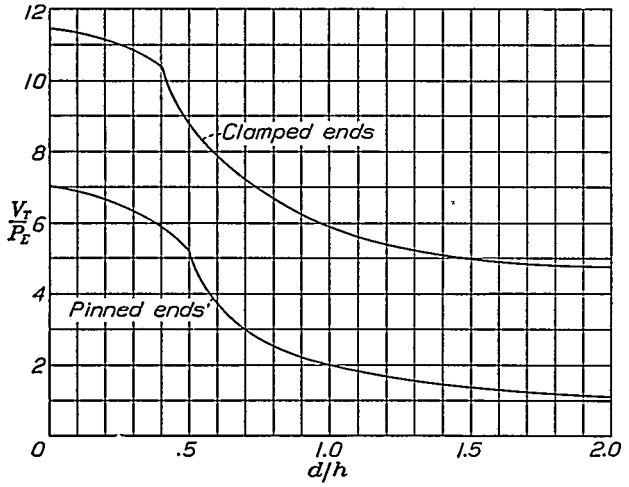

FIGURE 6.--Relation between theoretical buckling loads V_T of uprights and Euler loads. $P_E=\pi^2EI/h^2$ (from reference 1).

pute the effective column length L from the formula

$$L=h\sqrt{\frac{P_E}{V_T}} \tag{19}$$

With this effective length, the effective slenderness ratio L/ρ can be computed; the allowable stress is then obtained from the appropriate column curve.

The buckling of uprights in incomplete diagonal-tension fields is a very complex phenomenon, and there is little hope that theoretical solutions will be obtained in the near future. The following approximate method is therefore suggested:

The bracing effect of a web in pure diagonal tension on an upright with pin ends is measured by the difference V_T-P_E. The bracing effect of an elastic foundation is very nearly proportional to the foundation modulus (reference 4); the foundation modulus of the web is proportional to the diagonal tension and may therefore be assumed to be proportional to the diagonal-tension fraction k, if the bending stiffness of the sheet is neglected. For an incomplete diagonal-tension field, the bracing effect of the web might therefore be assumed to be $k(V_T-P_E)$. The tests by Limpert (reference 19) discussed in the second part of this paper suggest, however, that this estimate may be too optimistic. Until more extensive test data are produced to justify the assumption just made, it seems advisable to use a more conservative one. The assumption that the bracing effect is proportional to $k^2(V_T-P_E)$ gives a reasonably close approximation to Limpert's tests, as will be shown later. With this assumption, the effective column length to be used in computing the slenderness ratio becomes

$$L=\frac{h}{\sqrt{1+k^2D}} \tag{20}$$

where

$$D=\frac{V_T}{P_E}-1$$

In Limpert's test report, no mention is made of actual failures. It is therefore possible that failure to realize the full bracing effect proportional to k was only apparent and was caused by stopping the tests too early.

If the uprights are assumed to have some end fixity, the Euler load P_E in the expression for D must be replaced by the column load corresponding to the assumed fixity and h must be replaced by the effective length of a free column corresponding to the assumed fixity; for instance, if the fixity coefficient is assumed to be 4, then

$$D=\frac{V_T}{4P_E}-1$$

and

$$L=\frac{h}{2\sqrt{1+k^2D}}$$

Twisting failure of columns attached to a web was treated in reference 18 on the assumption that the sheet forces the center of twist of the column into the plane of the web. Undoubtedly the web also tends to aid the upright against twisting by virtue of having bending stiffness and by virtue of being under diagonal tension, although this effect may be small in many cases because uprights susceptible to failure by twisting are usually attached by a single row of rivets incapable of transmitting high torques from the web to the upright. There appears to be no published theory that takes the effect into account.

Failure by local buckling or crippling has been theoretically treated for a number of simple cross-sectional shapes; the most important types for the present purpose are treated in reference 20.

Thus far, mention has been made only of the stabilizing effect exerted by the web on the uprights. Unfortunately, there is also an opposite effect. The theory assumes the diagonal-tension folds to be very small. In fact, however, these folds are quite large; test experience has shown that, in most cases, one fold begins at each upright of a beam. The wave lengths of these folds are therefore comparable in order of magnitude with the wave lengths corresponding to primary and secondary column failure, and the folds tend to hasten the appearance of column failure in the uprights. Apparently no theory has been published that describes this premature forcing of failure.

Qualitatively, it is clear that the forces exerted by the web folds on the uprights convert the problem of upright failure from a pure stability problem into a stress problem; the case is analogous to the problem of columns with side load or with eccentric loading compared with centrally loaded columns.

II. EXPERIMENTAL INVESTIGATIONS

N. A. C. A. STRAIN-GAGE TESTS—SPECIMENS, PROCEDURE, AND ACCURACY

In order to appraise the validity of the proposed theory of the incomplete diagonal-tension field and in order to establish the value of the exponent n in equation (9), two beams were built and tested by the N. A. C. A. The pertinent dimensions of these beams are given in figure 7; figure 8 gives a general view of the test set-up. The two beams will be designated by their depths the 20-inch beam and the 10-inch beam.

Figure 9 shows a test set-up of the 20-inch beam with 2-inch Tuckerman gages on five uprights and 1-inch Tuckerman gages on the flange above two uprights. This figure also shows part of the structure used to provide lateral stability, the horizontal trussing being hidden from view behind the beam. Figure 10 shows an early set-up of the 10-inch beam.

The web and the flanges were 17S-T aluminum alloy and the uprights were 24S-T aluminum alloy. The uprights were interchangeable so that their spacing could be varied and different types of upright could be used. The two types of upright used for strain measurements are shown in figure 11. It will be noted that the uprights were always symmetrically arranged about the web; strains were always measured on both sides with opposing gages and the compressive strains in the uprights were obtained by averaging corresponding strains. The superposed bending strains and stresses caused by unavoidable eccentricities in the uprights may be considered as secondary effects analogous to the secondary stresses in trusses with rigid joints, that is, the term "secondary" does not necessarily imply that they are negligible.

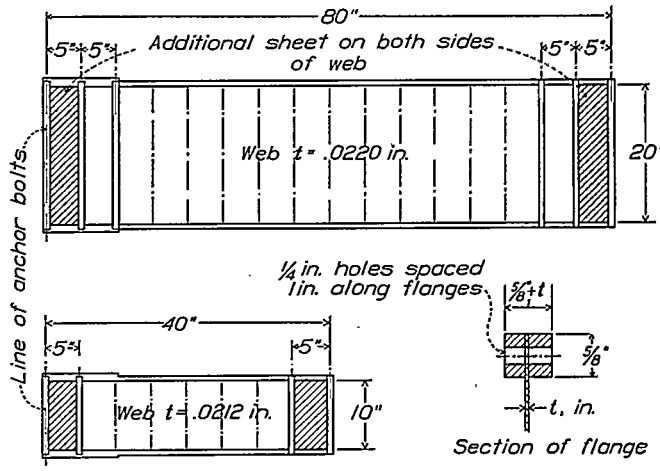

FIGURE 7.—Diagonal-tension test beams.

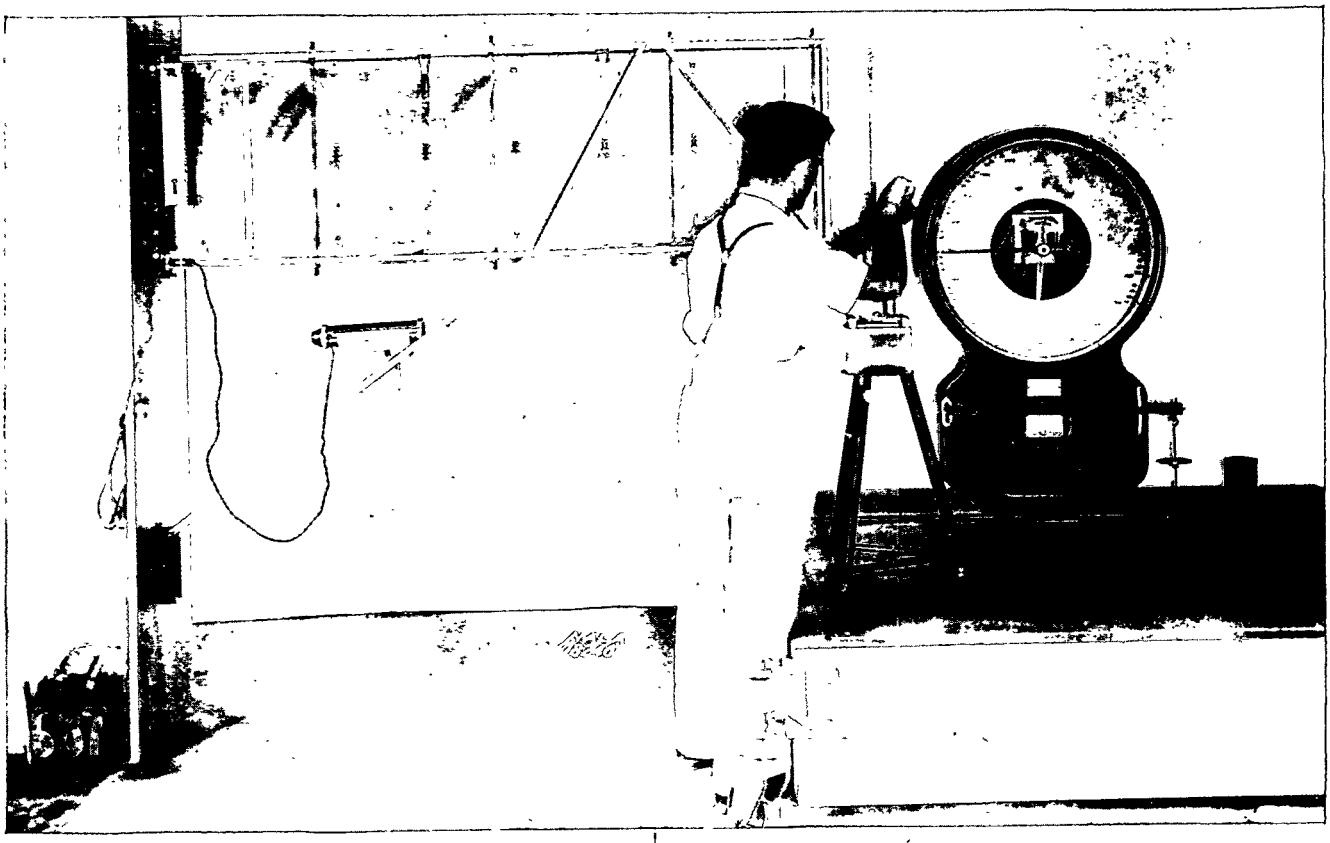

FIGURE 8.—General view of test set-up on N. A. C. A. 20-inch beam.

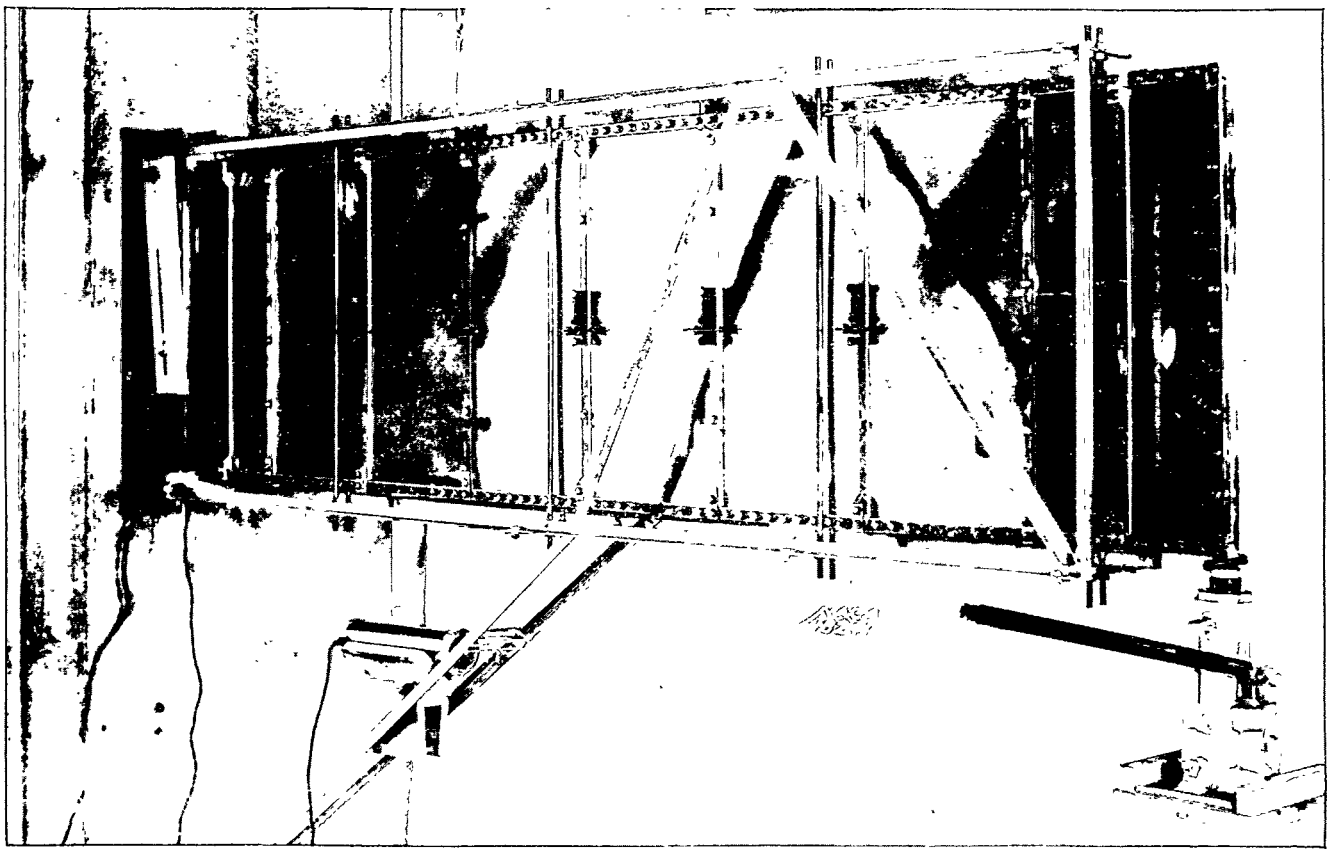

FIGURE 9.—Test set-up on N. A. C. A. 20-inch beam with alternating uprights.

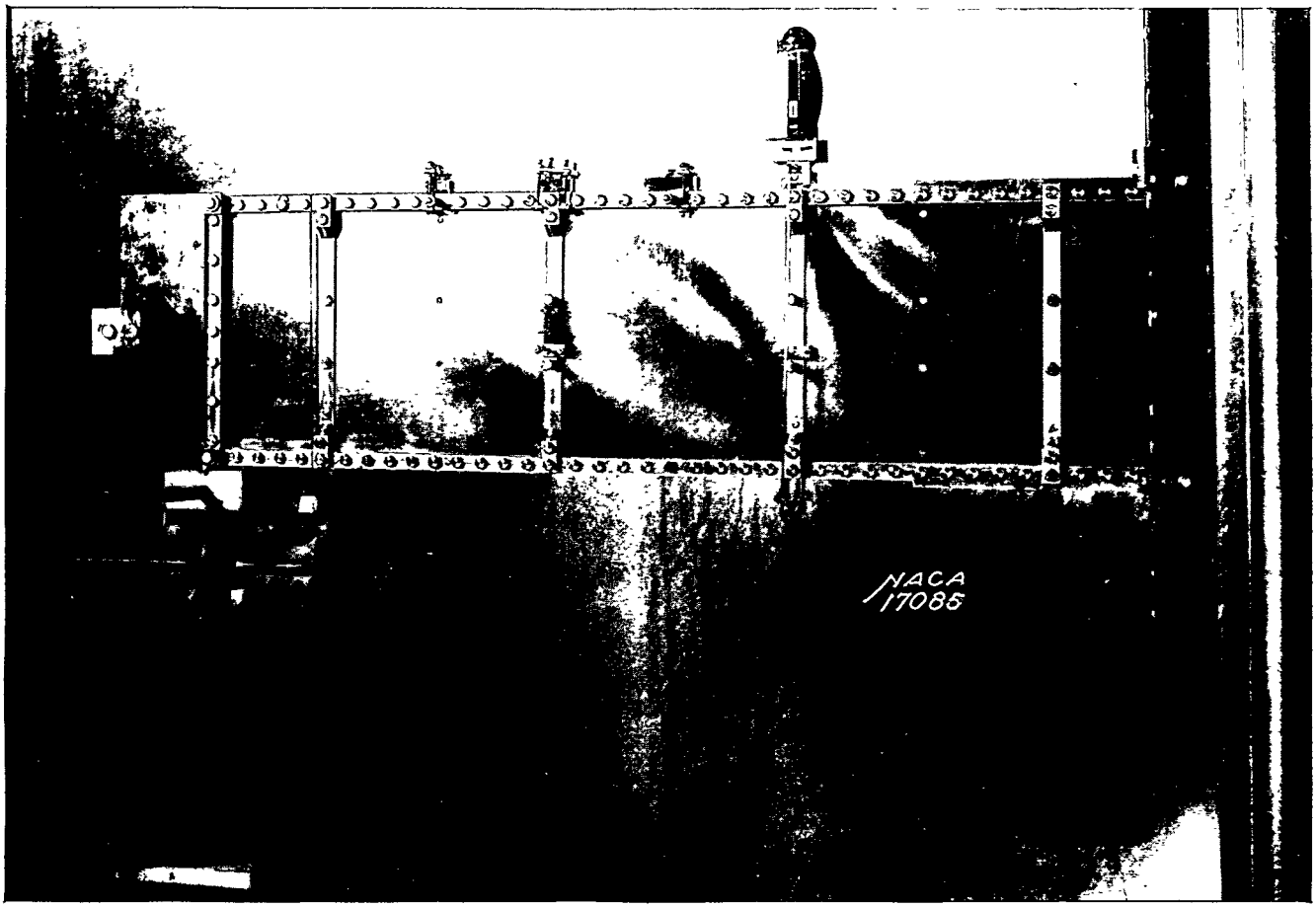

FIGURE 10.—Test set-up on N. A. C. A. 10-inch beam.

Figure 11 shows both types of upright in a somewhat peculiar arrangement (b) that calls for some explanation. In order to vary the critical stress without changing the general arrangement of the beam and also in order to obtain some idea of the effect of preventing buckling of the web in the immediate vicinity of the uprights, some tests were made on the 10-inch beam with the web entirely free from the uprights. The set-up for these tests was accomplished by using bolts and spacer tubes to connect the two parts of each upright; the web was pierced by holes sufficiently large to clear the spacer tubes.

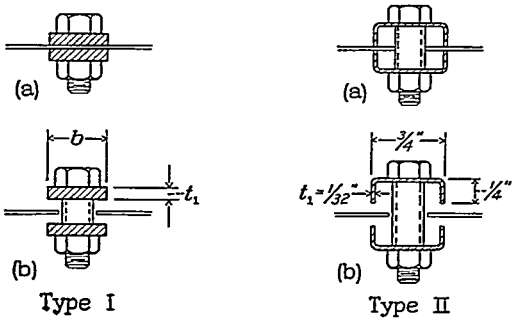

FIGURE 11.—Uprights for diagonal-tension beams.

Beam	Type I t_1 (in.)	Type I b (in.)	Type I Area (sq in.)	Type II [a] t_1 (in.)	Type II [b] Area (sq in.)
20-in	0.131	0.579	0.0758	1/32	0.0345
10-in	.129	.625	.0806	1/32	.0346

[a] Nominal thickness.
[b] Determined by weighing.

Tuckerman optical strain gages of 2-inch gage length were used on the uprights. The same type of gage was used on the flange in a few cases but, in general, Tuckerman gages and Huggenberger gages of 1-inch gage length were used on the flanges because the secondary bending stresses vary from a positive maximum to a negative maximum within a distance of half the spacing of the uprights. The Huggenberger gages were used in pairs, back to back, and their results were averaged because sometimes considerable differences of stress were found between the two halves of the flange. The Tuckerman gages had, in effect, three-point support and automatically eliminated this trouble, as was found by check tests against the Huggenberger gages.

All tests were repeated once and averaged. The repeat tests agreed, in general, to within about 100 pounds per square inch with the first tests, although differences of 200 pounds per square inch sometimes occurred; larger differences were rare. The differences between presumably identical stations, however, were sometimes very large. For this reason, the graphs showing stresses in the uprights give the group average of all the uprights tested on a given beam as well as the maximum compressive stresses measured. It should be kept in mind that all experimental upright stresses, including the maximum values shown, represent compressive stresses in the median plane obtained by averaging opposing gages, never individual stresses obtained from a single gage.

The smallest stress reading is 20 pounds per square inch on a 2-inch Tuckerman gage, 40 pounds per square inch on a 1-inch Tuckerman gage, and 100 pounds per square inch (estimated) on a Huggenberger gage. The temperature error, which amounts to about 50 pounds per square inch per degree Fahrenheit, was kept small by keeping the room temperature constant within about 1° F. Errors in load may be as much as 1 percent at loads above 1,000 pounds and somewhat higher at lower loads; these errors were caused by creep in the test set-up that sometimes occurred while strain readings were being taken.

For purposes of reference, table I is included as a key chart of the main tests. Each test is designated by a double number. The first number, either a 20 or a 10, identifies the beam as being either the 20-inch or the 10-inch beam; the second number designates the type of upright and the spacing of the uprights.

STRESSES IN UPRIGHTS OF N. A. C. A. 20-INCH BEAM

Stresses in uprights at midheight.—Figure 12 shows the stresses measured in the uprights of the 20-inch beam and the stresses predicted by using figure 4. The crosses denote the group average of the stresses in the uprights, the "group" including all the uprights on which strains are measured as indicated on the small sketches of the beam. The circles give the maximum compressive stresses measured.

The critical stresses for the sheet were computed by formula (16), assuming clamped edges except in the case of the channel uprights where the stress τ_{cr} was calculated on the assumption that the two edges of the sheet along the channel uprights were simply supported.

The break in the course of the experimental points for set-up 20–1 was caused by lateral failure of the flange. The test had to be stopped and additional lateral supports had to be added before the test could be continued to higher loads.

A rather significant comparison may be made between the results of set-ups 20–6 and 20–7. After the first test had been completed, the uprights were unbolted and uprights of type II were bolted on where uprights of type I had been, and vice versa. For all practical purposes, then, the two set-ups were identical and the physical structure was the same. In spite of this fact, the stresses measured in the uprights of type I in the first test were very much higher than the calculated stresses (fig. 12 (f)); whereas, the stresses measured in the second test agreed quite well with the calculated stresses (fig. 12 (h)). The absolute magnitude of the

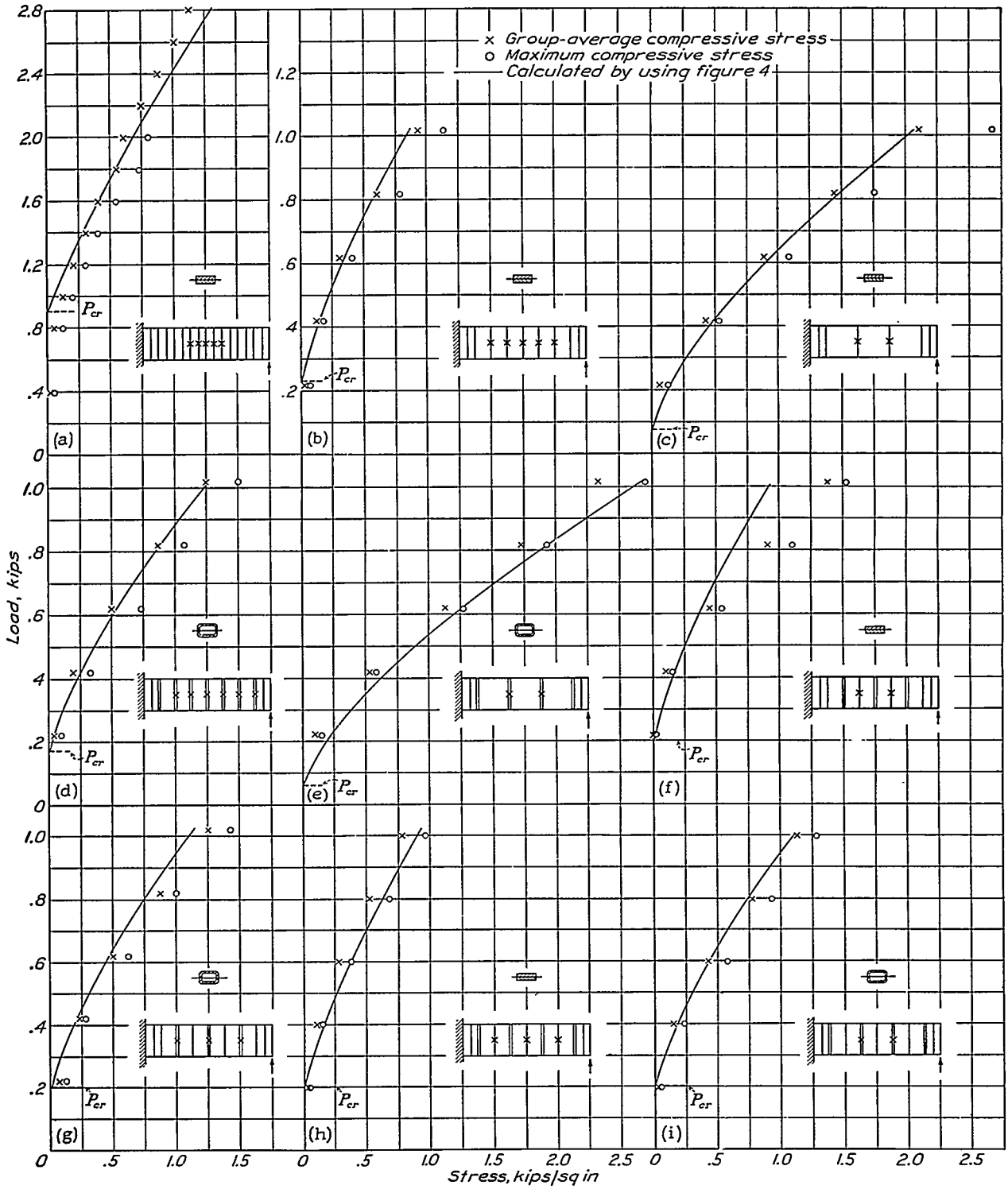

(a) Solid uprights, set-up 20-1. (b) Solid uprights, set-up 20-2. (c) Solid uprights, set-up 20-3.
(d) Channel uprights, set-up 20-4. (e) Channel uprights, set-up 20-5. (f) Solid uprights, set-up 20-6.
(g) Channel uprights, set-up 20-6. (h) Solid uprights, set-up 20-7. (i) Channel uprights, set-up 20-7.

FIGURE 12.—Stresses in uprights of N. A. C. A. 20-inch beam

stresses was rather low but the tests on set-ups 20–6 and 20–7 appear to be quite reliable, as indicated by the relatively small spread between group average and maximum stresses. The only possible conclusion is that stress differences of 20 or 30 percent can be caused in diagonal-tension beams by circumstances beyond any reasonable shop control.

Aside from this "wild" test, however, the agreement between calculated and observed strains is sufficiently uniform to validate the use of the proposed theory.

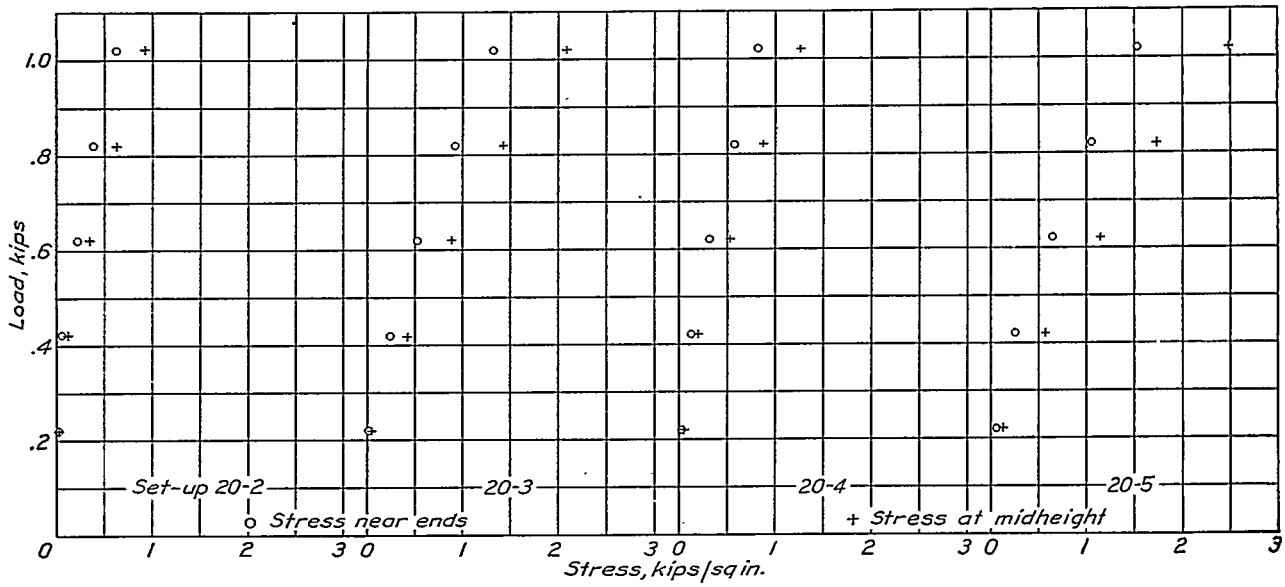

FIGURE 13.—Stresses in uprights of N. A. C. A. 20-inch beam at midheight and near ends.

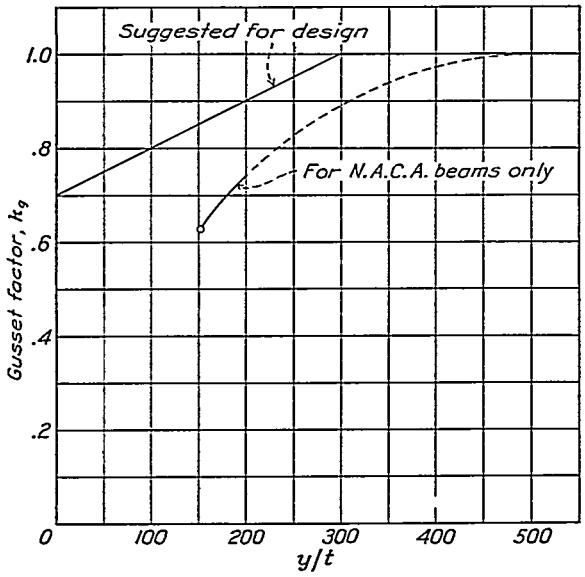

FIGURE 14.—Gusset factor, k_g.

Stresses near ends of uprights; gusset effect.—For set-ups 20–2 to 20–5, the stresses in the uprights were measured at stations 3.25 inches from the two flanges. Figure 13 shows these stresses as well as the stresses at midheight. It will be seen that a very consistent relation exists between these stresses, the stress near the end being on the average 0.62 times the stress at midheight. This effect may be spoken of as a "gusset effect," explained by the fact that the sheet in the corner is effectively prevented from buckling and thus forms a corner gusset increasing the effective area of the upright.

Except possibly for very close spacing of the uprights, the gusset effect probably depends primarily on the ratio y/t, where y is the distance of the station on the upright from the nearest flange. If this assumption is true, the effective size of gusset is constant for a given sheet thickness. Consequently, if the sheet thickness is kept constant and the depth of the beam is decreased, a point will be reached where the gusset extends to the midheight and then across this line; for shallow beams, then, the stress at midheight will be affected by the gusset. The theory of gusset effect may be put on a quantitative basis by assuming that equation (13) gives the stress when the ratio y/t is very large; for small ratios of y/t, this stress must be multiplied by a gusset factor k_g less than unity. Figure 14 is a curve of gusset factor against y/t based on the measurements of figure 13 and on the assumption that the factor approaches unity for $y/t=500$, which is about halfway between the values of $h/2t$ for the N. A. C. A. 20-inch beam and the Douglas beam to be discussed later. This curve is based on extremely meager data and consequently should not be used for design. It is shown only because it was used to estimate the gusset effect for the N. A. C. A. 10-inch beam to be discussed later; for this purpose, only the full-line part of the curve was needed. For design purposes, it is suggested that the conservative straight line indicated be used until more extensive tests establish the curve more securely.

The gusset effect probably also tends to reduce the stress σ_F in the flanges. The tests as made did not furnish the necessary information to evaluate these reductions. The practical importance of these reduc-

tions being very small in most cases, no undue weight penalty is paid for neglecting them in design work and using the full values of σ_F. A gusset effect also influences the secondary bending moments in the flanges, as will be shown later.

STRESSES IN UPRIGHTS OF DOUGLAS BEAM

Through the courtesy of the Douglas Aircraft Co., the inclusion here of the results of strain-gage measurements on a large diagonal-tension beam was made possible. A sketch of this beam is shown in figure 15; the lettered uprights indicate strain-gage stations. The

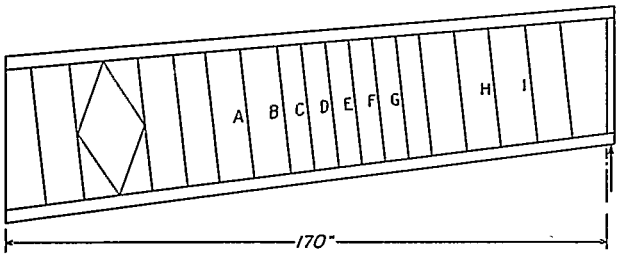

FIGURE 15.—Douglas test beam.

depth of the beam is about 40 inches near the middle of the beam and the web thickness is 0.036 inch. The value of h/t is therefore slightly over 1,000, or slightly higher than for the 20-inch N. A. C. A. beam. The beam gives a valuable extension of the test range in absolute size and particularly in stress. The maximum nominal shear stress on the N. A. C. A. beam was only about 6 kips per square inch, which is within the proportional limit; on the Douglas beam, the nominal shear stress varied because of taper between 15 and 18 kips per square inch in the region of the gage stations at a load of 23.4 kips, the highest loading at which strain measurements were taken. If the validity of formula (3) is assumed, the tensile stress in the web varied from 30 to 36 kips per square inch. Reference 21 gives, for 24S-T Alclad, a value of 27 kips per square inch as the proportional limit and of 37 kips per square inch as the yield point. The average stress in the web was therefore practically up to the yield point and, at the crests of the folds and other places of stress concentration, was beyond the yield point. According to the test report, definite permanent set had occurred in the web at a 20 percent smaller load.

Figure 16 shows the experimental and the calculated stresses of the Douglas beam. In view of the ever-present possibility of large inexplicable deviations, the agreement is, on the whole, quite satisfactory. Only at low loads is there a peculiar tendency for the observed stresses to be much higher than the calculated stresses.

STRESSES IN UPRIGHTS OF N. A. C. A. 10-INCH BEAM

Figures 17 (a) to 17 (c) show the stresses measured on the uprights of the 10-inch beam in the "web-clamped" condition; the crosses again indicate the group average of all measured stresses and the circles give the maximum stresses measured. The calculated stresses were obtained by using the design chart of figure 4 and multiplying the stresses with a gusset factor of 0.72 obtained from figure 14.

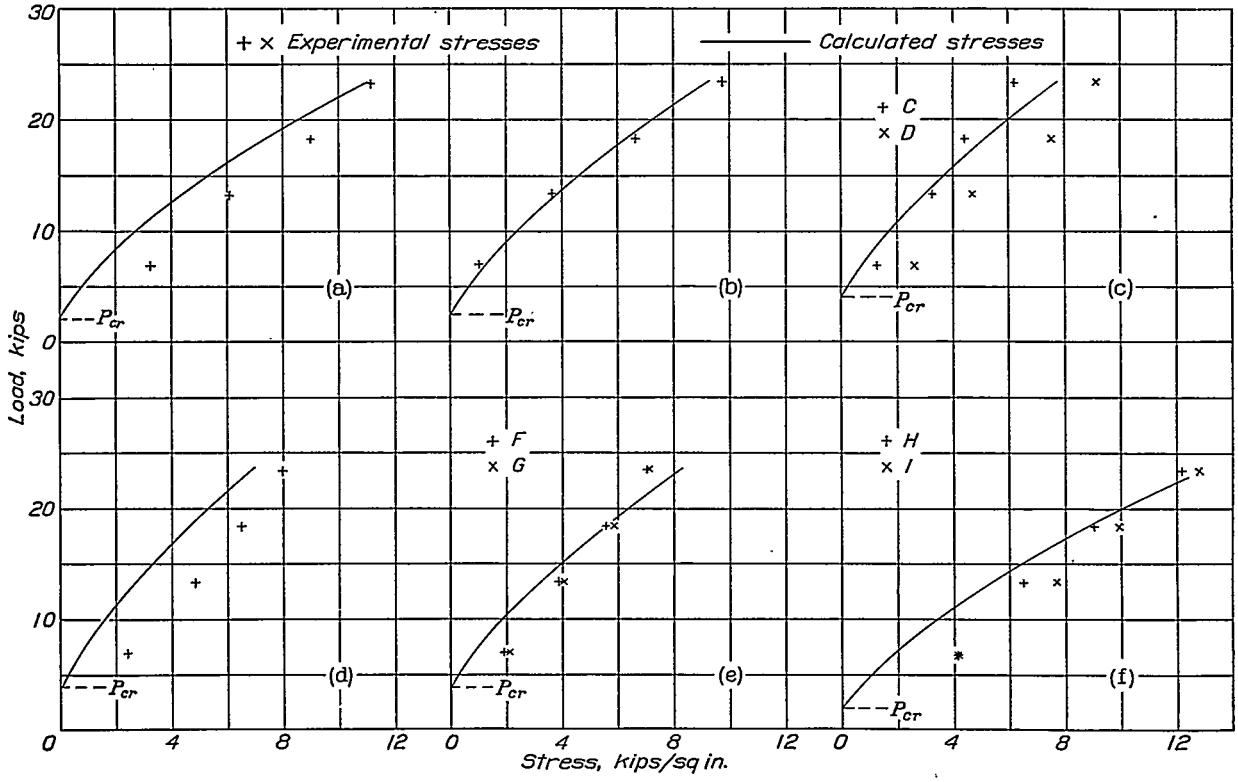

(a) Upright A. (b) Upright B. (c) Uprights C and D.
(d) Upright E. (e) Uprights F and G. (f) Uprights H and I.

FIGURE 16.—Stresses in uprights of Douglas test beam.

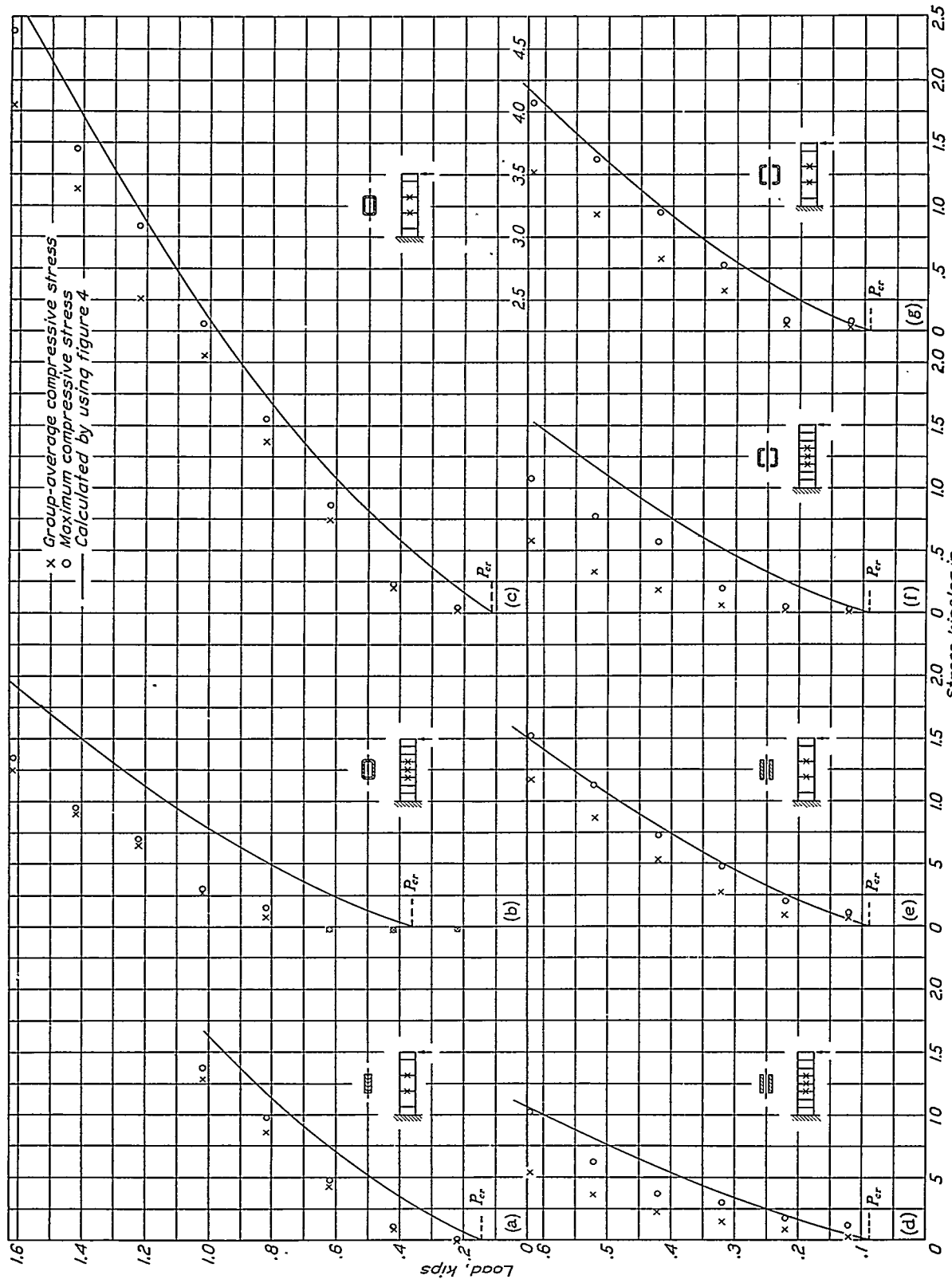

(a) Set-up 10-1. (b) Set-up 10-2. (c) Set-up 10-3.
(d) Set-up 10-4. (e) Set-up 10-5. (f) Set-up 10-6. (g) Set-up 10-7.

FIGURE 17.—Stresses in uprights of N. A. C. A. 10-inch beam.

In all three cases (figs. 17 (a) to 17 (c)), the computed stresses are on the conservative side—that is, higher than the observed stresses, even when the maximum experimental stresses rather than group-average stresses are used as the basis of comparison. On the basis of the maximum stresses, the average difference for all three tests between computed and observed stresses is about 20 percent; on the basis of group-average stresses, it is about 27 percent. Comparison with the results for the 20-inch beam indicates that a lower value of h/t permits the bending stiffness of the sheet to play a relatively greater part and to delay somewhat the development of the diagonal-tension field; equation (10) should therefore probably contain a factor involving h/t. The existing data are too few to establish this factor; but it may be concluded that, when h/t is about 500, the calculated stresses are sufficiently conservative to be taken as the maximum upright stresses rather than as group average upright stresses.

Figures 17 (d) to 17 (g) show the stresses measured in the uprights of the 10-inch beam in the "web-free" condition. The stresses calculated by using figure 4 fit the maximum stresses reasonably well but are very conservative compared with the group-average stresses. It should be noted that the free web acts in a very nonuniform manner, the maximum upright stresses amounting to nearly twice the group-average stresses. It is therefore difficult to compare the accuracy of calculating the web-free condition with the accuracy of calculating the web-clamped condition. Under any condition, however, the calculations for the 10-inch beam are more conservative than the calculations for the 20-inch beam with its larger h/t ratio.

SECONDARY BENDING MOMENTS IN FLANGES OF N. A. C. A. BEAM

The flange stresses were measured in the two N. A. C. A. beams at the outside fiber of the compression flange. These stresses arise by superposition from three individual sets of stresses: the primary beam stresses σ_B, the compression stresses σ_F caused by the horizontal component of the diagonal tension in the web, and the secondary bending stresses σ_{SB} caused by the distributed vertical component of the diagonal tension.

The primary beam stresses σ_B at a station x inches from the tip were computed by the ordinary beam formula

$$\sigma_B=\frac{Px}{Z}$$

where Z is the section modulus of the entire beam. For the computation of the section modulus of the beam, the material active in bending was assumed to be the material indicated by cross hatching on the cross sections shown in figure 3. Deduction of the beam stresses from the observed stresses yielded the stress differences ($\sigma_{observed}-\sigma_B$) shown in figures 18 (a) and 18 (b). The compressive stresses σ_F were then computed by formula (14). By deduction of σ_F from the stress differences ($\sigma_{observed}-\sigma_B$) the secondary bending stresses σ_{SB} were obtained as indicated in figures 18 (a) and 18 (b) for the maximum loads.

Comparison of the stresses σ_{SB} in figures 18 (a) and 18 (b) shows that the secondary bending stresses are higher between the uprights than at the uprights. In a continuous beam of constant cross section, the stresses between supports are lower than or, at the most, equal to the stresses at the supports. The observed relation between the stresses can therefore be explained only by assuming that the previously discussed gusset effect increases the effective section modulus of the flange near the uprights. If the flange can no longer be considered as a beam of constant cross section, the coefficients k_M used in equation (5) must be changed.

In most practical cases, the secondary bending stresses are not sufficiently important to warrant the trouble of calculating the flange as a beam of variable cross section. A single moment coefficient $k_M=0.10$ was therefore chosen to represent the maximum bending moments in the flange, with the understanding that these moments occur between uprights but that the moments at the uprights may sometimes be practically as large as the maximum moments. The numerical value 0.10 was chosen because it is conservative for all experimental results and because it is reasonably close to the theoretical value of $\frac{1}{12}$ for the maximum moment in the limiting case of pure diagonal tension. When the secondary bending stresses are computed from the bending moments, the section modulus of the individual flange is computed for the cross-hatched area A_F indicated in figure 3, but an allowance should be made for rivet holes.

The secondary bending stresses σ_{SB} shown in figure 18 (a) were multiplied by the section modulus of the flange to obtain the secondary bending moments. For comparative purposes, moment coefficients defined by the equation

$$M=k_m S_{DT} d^2/h$$

were calculated from these moments and are plotted in figure 19 against the loading ratio. These coefficients k_m differ from the coefficients k_M because the flexibility factor C_1 has been taken as unity. Figure 19 shows that the moment coefficients generally increase with loading ratio, but it is probably safe to assume that the rate of increase will drop rapidly with somewhat higher loading ratios. Set-up 20–1 differs quite radically in having very high moment coefficients decreasing very rapidly. The loading ratios are low for this set-up, and the trend of the moment coefficients is probably not typical but falsified by accidental sources of error that play a relatively large part at low loading ratios, as shown throughout these tests.

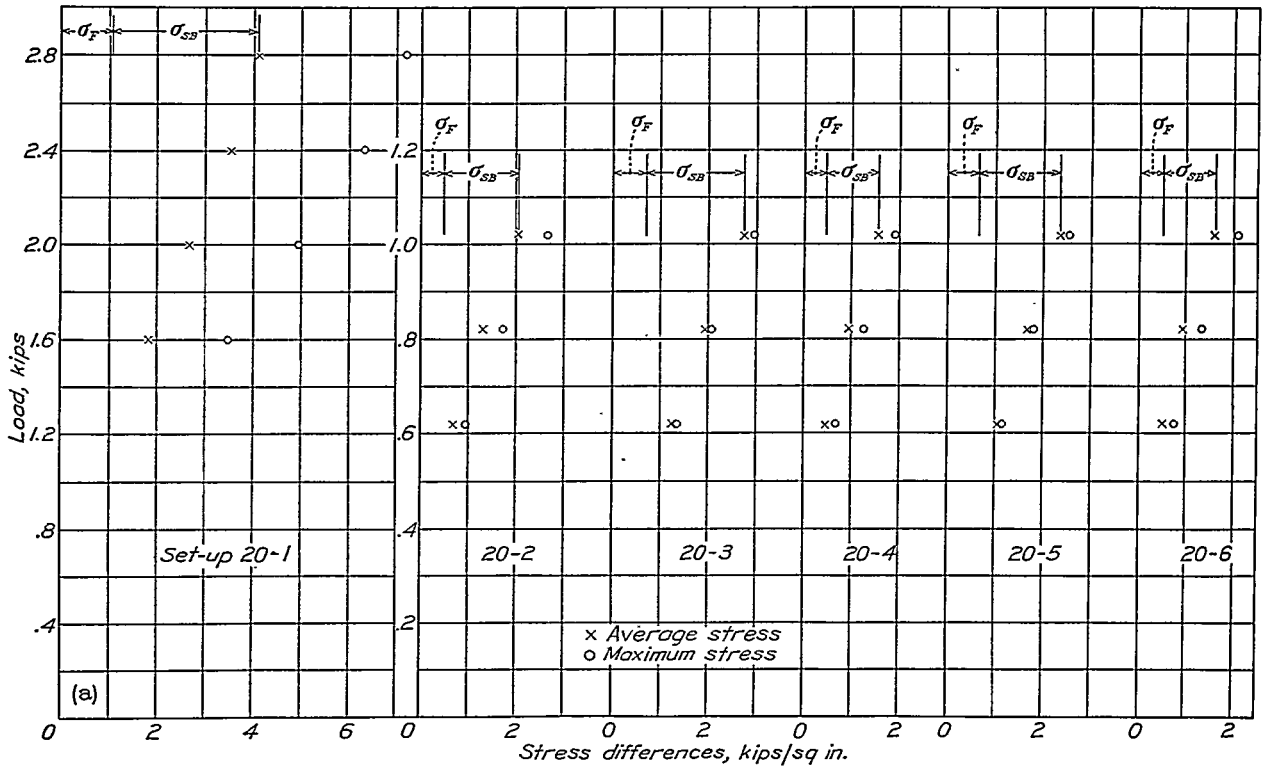

(a) At stations between uprights.

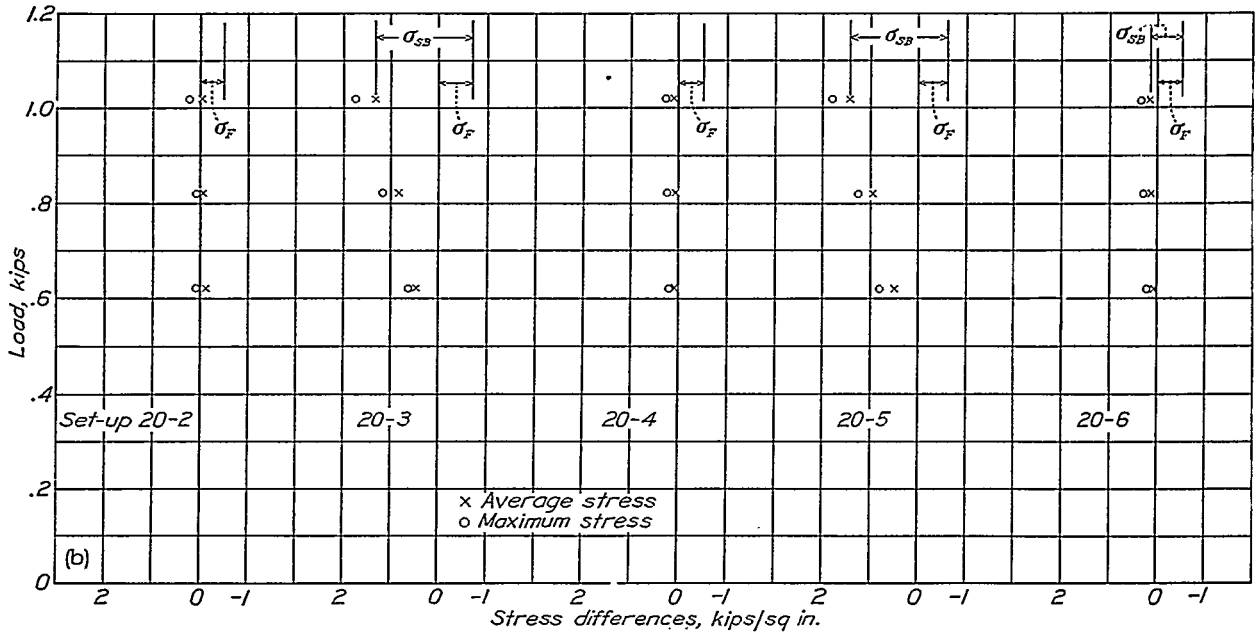

(b) At stations over uprights.

FIGURE 18.—Stress differences ($\sigma_{observed} - \sigma_B$) in compression flange of N. A. C. A. 20-inch beam

For the highest load used on each set-up, the experimental values of k_m were divided by the chosen standard value $k_M=0.10$ in an attempt to check experimentally the influence of the flexibility parameter ωd. Figure 20 shows the results. Taken in conjunction, figures 19 and 20 indicate that the formula

$$M=0.10\ C_1 S_{DT} d^2/h \qquad (21)$$

gives, in general, very conservative values for the secondary bending moments in the compression flanges

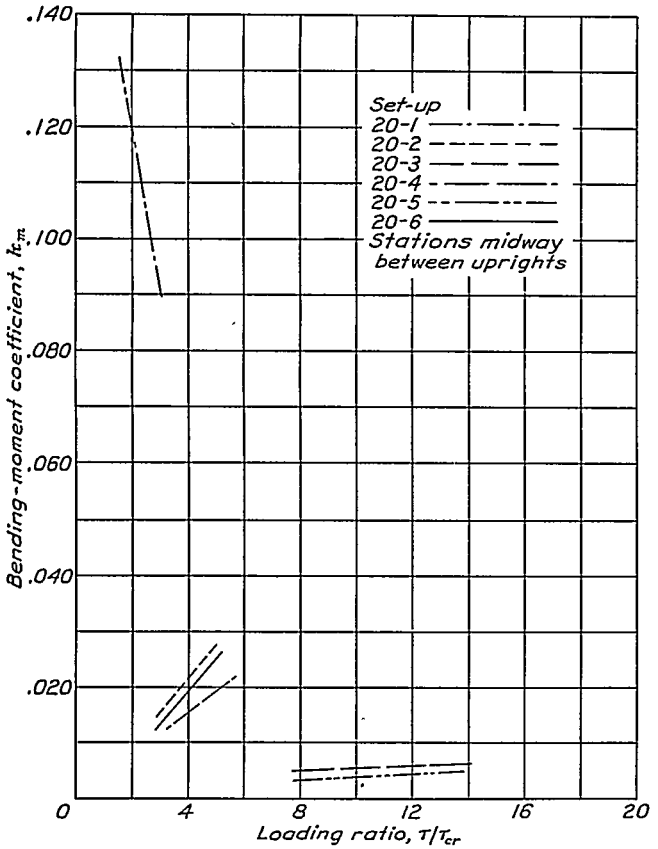

FIGURE 19.—Change of bending-moment coefficient with loading ratio for N. A. C. A. 20-inch beam.

at low loading ratios; as the loading ratio increases, the formula becomes less conservative, but it will probably never become unconservative, assuming of course that the comparison is made with average experimental values and not with individual high values.

On set-ups 20–1, 20–2, and 20–3, the secondary bending moments were obtained on the tension flange of the beam for the same maximum loads that had been used for the measurements on the compression flange. The secondary moments were, respectively, 25, 16, and 41 percent of the corresponding moments on the compression flange. These differences are explained as follows: The tension delays development of the folds near the flange, and a strip of the web adjacent to the flange remains plane. This strip adds to the moment of inertia of the flange and helps the flange to carry the secondary moments. Obviously, the magnitude of the help increases with the ratio of tension stress to shear stress and decreases with increasing loading ratio.

A number of measurements were made on the compression flange of the N. A. C. A. 10-inch beam. All the bending-moment coefficients obtained from these measurements were considerably below the coefficients obtained for the 20-inch beam; it was therefore considered not worthwhile to show them.

BUCKLING OF THE WEB SHEET

The coefficients K given in figure 5 for calculating the critical stress of the sheet apply, strictly speaking, only when the sheet is in pure shear. Actually, the sheet is also subjected to bending stresses but, in diagonal-tension beams designed for high structural efficiency, the effect of the bending stresses on the critical stress can probably always be neglected.

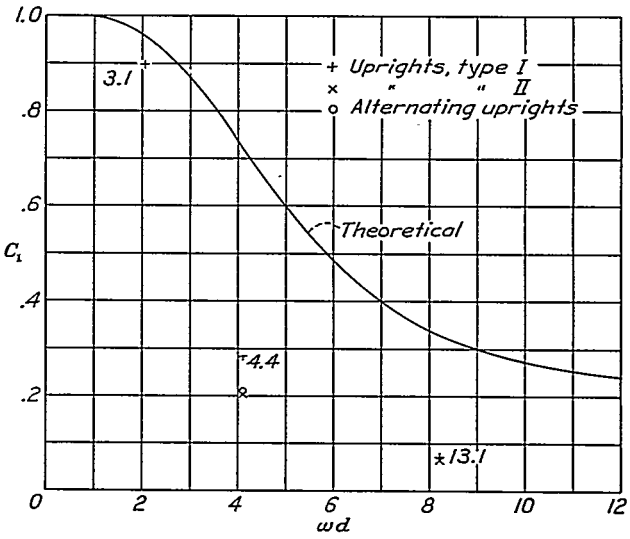

FIGURE 20.—Experimental and theoretical influence of flexibility of flange on secondary bending moments in compression flange of N. A. C. A. 20-inch beam. Values near test points are average values of τ/τ_{cr}.

This simplifying circumstance is due to the fact that the critical stress is of little interest in itself and consequently need not be very accurately known; it is needed only to compute the diagonal-tension fraction k.

Special buckling tests made by a number of investigators have shown that, with sheet of ordinary flatness and test jigs of ordinary dimensions, the buckling of sheet subjected to pure shear usually starts at 60 to 80 percent of the theoretical critical load. Very careful tests have shown that buckling may be delayed to loads of about 90 percent of the critical by using very flat sheet and very heavy test jigs. The deflections are quite small at first, however, and sensitive means of measuring must be employed to detect them.

On diagonal-tension beams, the buckling of the web begins on the compression side of the beam and carries across the neutral axis for some distance. Near the tension flange, buckling is delayed by the stiffening action of the tension.

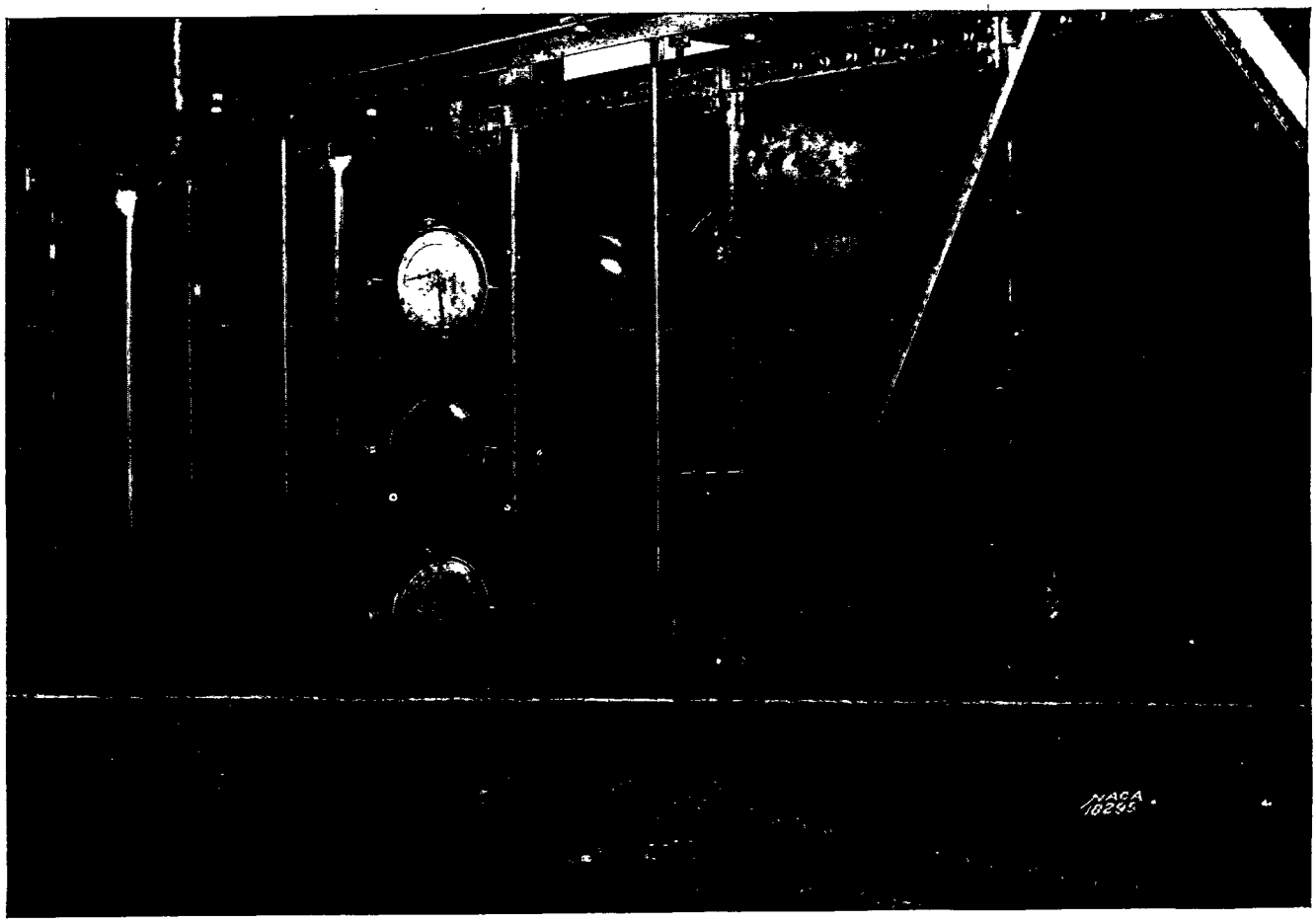

FIGURE 21.—Set-up for measuring buckling deformations of uprights on N. A. C. A. 20-inch beam.

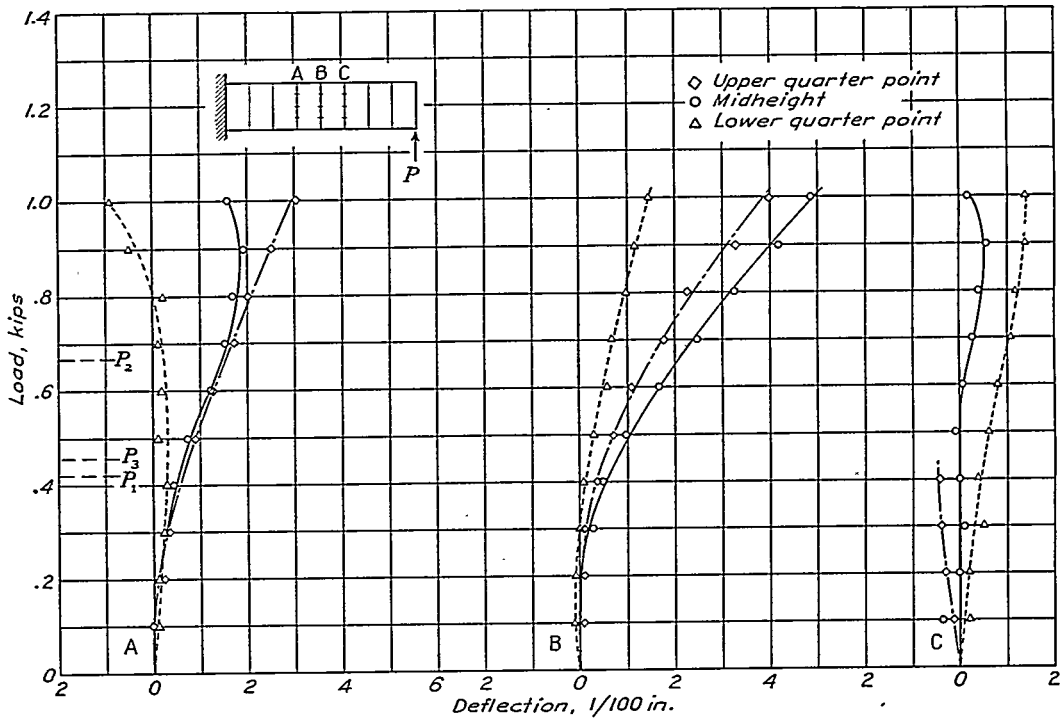

FIGURE 22.—Deflections of uprights on N. A. C. A. 10-inch beam.

In the tests of the N. A. C. A. beams, no special instruments were used to detect the beginning of buckling of the web. With ordinary visual inspection, the first buckles were usually detected at about 150 percent of the calculated critical load. By means of a straight-edge laid across the sheet, the first buckles could usually be detected at about 120 percent of the critical load.

An indirect and therefore not very accurate check on the buckling of the sheet was furnished by the strain measurements on the uprights of the N. A. C. A. beams; the first appearance of stresses in the uprights should coincide with the first buckling of the sheet. Considering the weaknesses of this indirect method of checking, the agreement indicated by the inspection of figures 12 and 17 is fair.

EXPERIMENTS ON THE BUCKLING OF THE UPRIGHTS

Tests of N. A. C. A. beams.—The main purpose of the N. A. C. A. tests was to study the stress distribution in incomplete diagonal-tension fields. Some exploratory tests, however, were made on the problem of buckling of the uprights. Figure 21 shows the set-up of the 20-inch beam. The bridge carrying the dial gages was provided with knife edges resting in the corner between web and flange. The dial gages gave the deflections of the uprights at the upper and the lower quarter points and at midheight. The set-up for the 10-inch beam was similar.

The uprights used on the 10-inch beam were similar to the uprights of type I but were only $\frac{1}{16}$ inch thick. Figure 22 shows the measured deflections plotted against the applied load. Three calculated critical loads are indicated: P_1 is the critical load for general elastic instability calculated by equation (17), supported edges being assumed; P_2 is the critical load for general instability calculated by equation (17) after changing the coefficient 17.5 to 27.8, clamped edges being assumed; P_3 is the critical load causing buckling of the sheet between uprights. In this particular case, instability of the sheet and general instability of the web begin at about the same load. The half-wave length corresponding to P_1 is $\lambda_1=8.2$ inches; corresponding to P_2, it is $\lambda_2=5.5$ inches. The theory of anisotropic buckling is therefore just barely applicable because the spacing of the uprights is 5 inches. At some stations, the experimental curves show deflections beginning at very low loads and, in general, the experimental curves are of such shape that a buckling load cannot be defined with any degree of certainty; it seems justifiable to state, however, that the deflections became noticeable in the neighborhood of the predicted critical loads.

Two sets of deflection measurements were taken on the N. A. C. A. 20-inch beam. In both tests, uprights of type I were used. In the first test, the spacing was 5 inches; in the second test, 10 inches. Figures 23 and 24 show the measured deflections. The half-wave length for the first case is $\lambda_1=10.5$ inches; for the second case, $\lambda_1=12.5$ inches. The theory may therefore be considered applicable in the first case but not in the second case. As on the 10-inch beam, the shape of the curves is such that it is impossible to define definitely any point on them as the buckling point, but the deflections become appreciable in the neighborhood of the calculated critical load.

The general shape of the observed deflection curves confirms the conclusion previously drawn that the buckling of the uprights is not a pure stability problem but a stress problem, because initial eccentricities and interaction with web folds cause deflections to begin practically as soon as load is applied. At the calculated critical load S_{cr}, the deflections of the N. A. C. A. beams are 0.06 to 0.11 percent of the length of the uprights; the deflections vary roughly as the square of the load.

Limpert's tests.—Limpert (reference 19) tested four diagonal-tension fields with closely spaced and very flexible uprights (L/ρ from 340 to 550). The load was not applied as beam load; a parallelogram was used to load the specimens in pure shear. As a result of this method of testing, it was easy to measure the angles of shear strain, which Limpert gives as the main results of his tests. As the criterion for buckling, he chose the load at which the curve of shear strain against load departs from the straight line.

A closer examination of the tests shows that the web stresses were rather high, so that yielding of the web material might have been not only a contributing cause but possibly the main cause for the departure from a straight line in the strain-load diagram. Very definite conclusions in this respect cannot be drawn because the physical properties of the web material (brass) are not given.

Limpert states that large buckles occurred at half the critical load calculated by him. Unfortunately, he gives only a few sample curves of deflection for one specimen, which are given for loads far beyond the critical load for anisotropic buckling; consequently, no check can be made at the critical load. On the assumption, however, that the square law of the increase of deflection holds, as noted on the N. A. C. A. beams, it is possible to find by extrapolating backward that the maximum deflections at the critical load for anisotropic buckling were about 0.04 to 0.06 percent of the length of the upright, which is of the same order of magnitude as the deflections on the N. A. C. A. beams.

The tests made by Limpert were used to obtain experimental confirmation of the bracing effect that the diagonal-tension web exerts on the uprights. The stresses developed in the uprights of Limpert's test specimens were computed by the use of the design chart given as figure 4; these stresses were multiplied by the cross-sectional areas of the stiffeners to obtain the loads carried in the stiffeners. From the lengths of

407300°—41——27

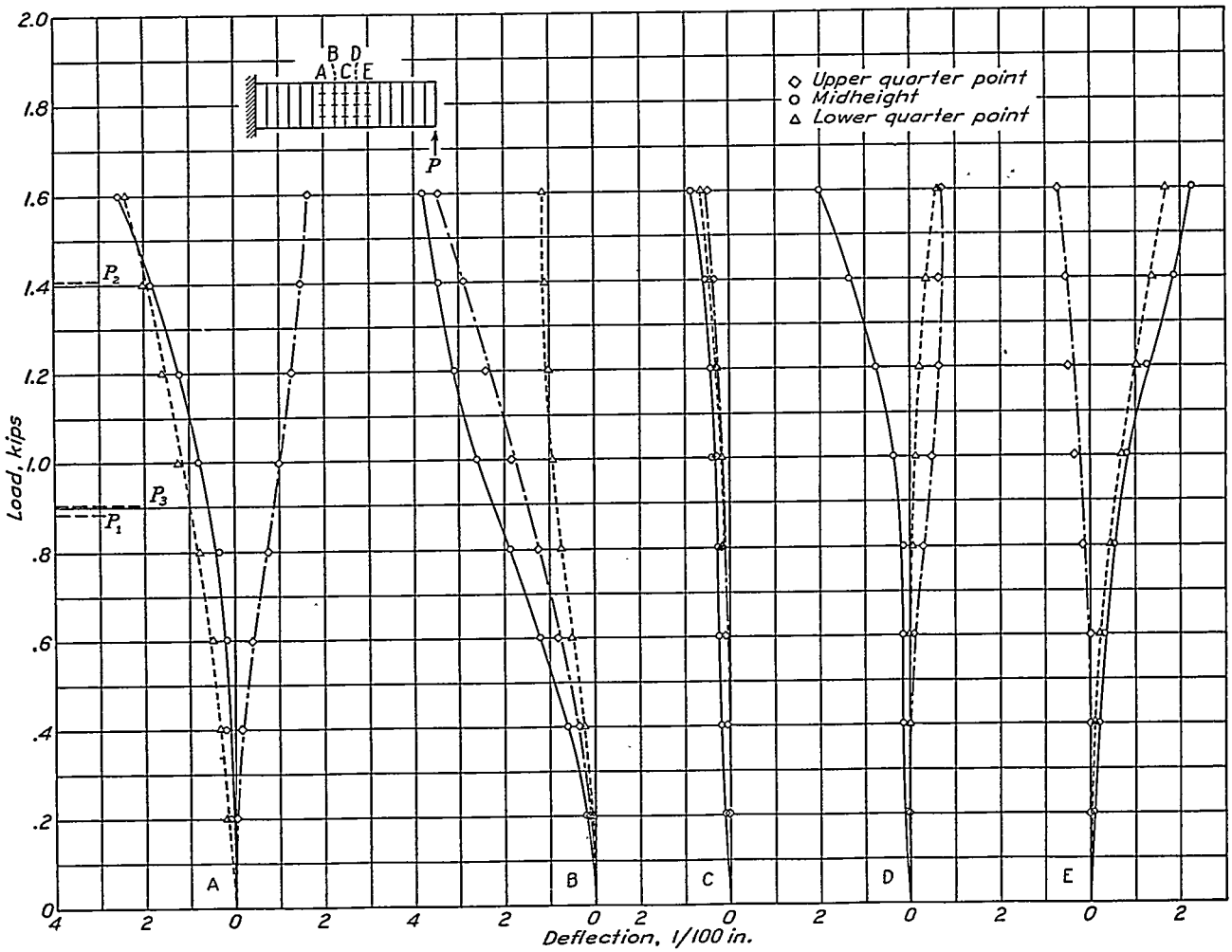

FIGURE 23.—Deflection of uprights on N. A. C. A. 20-inch beam with 5-inch spacing.

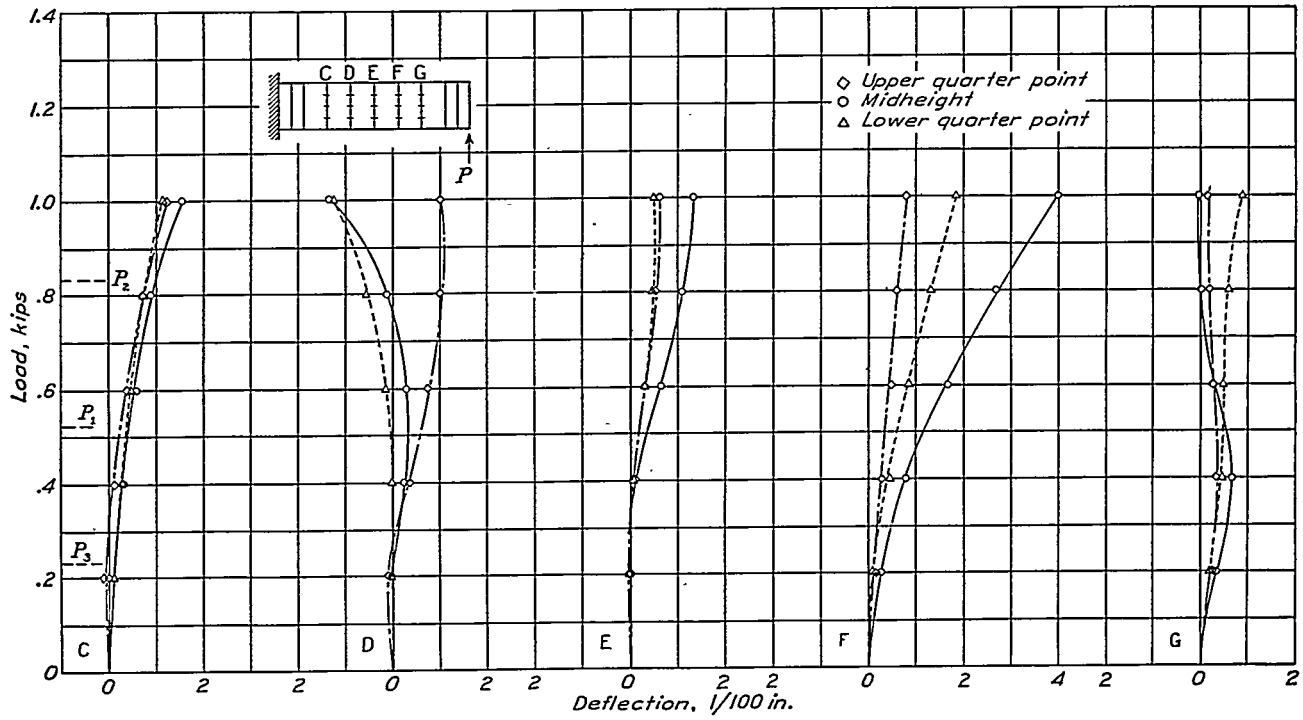

FIGURE 24.—Deflection of uprights on N. A. C. A. 20-inch beam with 10-inch spacing.

the uprights and their moments of inertia, the Euler stresses were then computed. The ratios of the developed stresses to the Euler stresses were listed in table II. The diagonal-tension fraction k was then computed and listed in table II. Next, the values $1+k^2D$ were computed in accordance with the proposed approximate method of estimating the buckling load in incomplete diagonal-tension fields and were listed in the table. The last column in the table gives the ratio of developed strength to predicted strength; the average ratio for the four tests is very close to unity.

TENTATIVE CONCLUSIONS ON BUCKLING AND STRENGTH OF UPRIGHTS

In addition to the experiments on buckling of uprights described in the preceding section, there are on file at the N. A. C. A. a number of routine test reports made by manufacturers and other agencies. Unfortunately, most of these reports are entirely useless, as far as correlation with theory is concerned, because important data are lacking; for instance, the moment of inertia of the uprights is usually omitted. Furthermore, the uprights were often overstrong and did not fail. There are, consequently, very few useful experimental data available. On the other hand, it was pointed out in part I that the theory of failure of uprights is not very well developed, particularly with reference to interaction between uprights and web. The following conclusions based on these routine tests as well as on the tests discussed in this paper should therefore be understood to be of a very tentative character.

The theory of buckling of an orthotropic plate under shear stress agrees reasonably well with the observed facts. Onset of this type of general elastic instability is, however, not a very obvious phenomenon, because the diagonal-tension folds in the web tend to cause the premature appearance of slight buckles and because initial buckles may exist. Experiments with corrugated sheet (reference 16) have shown very good agreement with the theoretical buckling loads.

If the uprights are sufficiently flexible to withstand large deformations, the load causing general elastic instability of the stiffened web can be safely exceeded. In Limpert's tests, the critical load was exceeded 2 to 6 times.

The stabilizing effect that a web in incomplete diagonal tension exerts on the bending failure of uprights can be estimated by using a fraction of the theoretical stabilizing effect of the pure diagonal-tension field proportional to the square of the diagonal-tension fraction k, as indicated by equation (20).

If the uprights have thin walls or legs subjected to local buckling failure, the stresses at which failure occurs are about equal to the stresses that would cause crippling if the uprights were tested as free columns, provided that the leg attached to the web is at least as thick as the web and the ratio A_U/td is not less than 0.3.

If the ratio A_U/td is less than 0.3, the sheet may take charge and force failures in the uprights. Under these conditions, there is probably little relation between the failing stresses of the uprights and the failing stresses of the corresponding free columns; tests appear to indicate that the failing stress of the upright may be less than half the failing stress of the free column.

The only theoretical design criterion for such cases is formula (17) for general elastic instability. If the upright spacing is within the usual limits ($d \leqq h/2$) and the uprights are of sufficiently compact cross section to eliminate local buckling, a small ratio A_U/td will necessarily indicate slender uprights. Under such conditions, the ultimate load for the few pertinent tests ranges between 1.7 and 2.5 times the critical buckling load given by formula (17). Only on corrugated sheet was the ratio found to drop as low as 1.2 (reference 16). It therefore seems safe to design webs having the ratio A_U/td below 0.3 so that the general elastic instability begins at the design yield load, which by definition is two-thirds of the design ultimate load, but there is no theoretical method of finding quantitatively the margin against ultimate failure.

STRESSES IN THE WEB

In an incomplete diagonal-tension field, the stress in the median plane of the web is a biaxial or a combined stress. Superposed on this stress are bending stresses caused by the formation of the folds. The direct determination of the stresses by means of strain measurements is hampered by practical obstacles that thus far have deterred investigators from making any measurements of this kind. Strain measurements can be quite easily made in a direction parallel to the folds, but this process is insufficient to determine all the components of the combined stresses. Measurements in directions not parallel to the folds are very difficult to make and to evaluate; they would require gages with a very small gage length or auxiliary measurements of sheet curvature.

In the N. A. C. A. tests, no attempt was made to measure strains in the sheet. The only measurements available are those given in reference 5 based on slope measurements on the sheet. According to these measurements, the stress σ_{id} in the median plane of the sheet is practically equal to 2τ even for a loading ratio of less than 2. This stress σ_{id} is an equivalent uniaxial or simple stress entailing the same danger of rupturing the sheet as the actual combined stress, assuming that the danger of rupture is measured by the amount of strain energy stored in an element of unit volume.

The maximum web stresses occur in the outer fibers of the sheet on the crests of the waves. In the tests reported in reference 5, these stresses were found to be 1.5 to 1.7 times the average web stresses for the loading ratios considered in this paper (below 40) and for practical values of σ_U/τ. These stresses occurred

midway between uprights. At loading ratios higher than 40, the maximum stresses were found near the edge of the sheet, where the folds are forced back into a plane by the edge members (cap strips). Only a few scattered test points are available and indicate stresses as high as 2.2 times the average web stress.

It might be mentioned that, in the tests of reference 5, the flanges were so stiff that the flexibility parameter ωd was practically zero and the factor C_2 of equation (3) was equal to unity.

III. STRESS ANALYSIS OF DIAGONAL-TENSION BEAMS

RANGE OF APPLICABILITY

The empirical coefficients of the proposed method of analysis were obtained by tests of beams having values of h/t from 500 to 1,000. The method may be expected to give good approximations for values of h/t beyond 1,000; as the value of h/t decreases, the method becomes increasingly conservative.

General test experience indicates a large scatter of test results at loading ratios τ/τ_{cr} below 3 or 4; the diagonal-tension effects consequently cannot be very closely calculated in this range.

All the test data on which the proposed method of analysis rests were obtained on beams with upright spacings $d \leqq h$. Consequently, the method should not be used for beams with $d > h$.

ANALYSIS OF THE FLANGES

The flanges are subjected to three distinct sets of stresses: the primary beam stresses computed by the standard beam formula or truss formula, the compression stresses σ_F that balance the horizontal component of the diagonal tension in the web, and the stresses caused by the secondary bending moments.

The stresses σ_F are computed with the help of formula (14).

The secondary bending moments are computed with the help of equation (21). These moments should be assumed to be of equal magnitude but of opposite sign at stations between uprights and at stations at uprights. Unless more extensive experimental data than given in this paper are obtained, the theoretical curve of figure 2 should be used for C_1 and the moments on the tension flange should be taken to be as large as the moments on the compression flange. It can probably be assumed that secondary bending moments computed in this manner are always conservative.

The secondary bending stresses σ_{SB} in the flanges are obtained by dividing the secondary moments by the section moduli of the individual flanges. The section moduli should be computed assuming the material effective in bending to be the cross-hatched area A_F shown in figure 3. An allowance should be made for rivet holes; no allowance should be made for gusset effect, because this effect is already taken into account by the method of computing the moments.

ANALYSIS OF THE WEB

According to the measurements of reference 5, the maximum stresses in the outside fibers of the web are about 1.5 to 1.7 times the stresses in the median plane of the web for loading ratios below 40. The first indications of yielding and permanent set may therefore be expected when the stress in the median plane of the web $\sigma = 2\tau/C_2$ is between 1/1.7 and 1/1.5 $\sigma_{y.p.}$ or between 0.59 and 0.67 $\sigma_{y.p.}$. Although the implied use of the particular equivalent stress σ_{id} of reference 7 is open to debate, possible changes in equivalent stress will be of little importance compared with the practical difficulty of determining in a built-up structure the load at which yielding and set first appear. For loading ratios above 40, reference 5 indicates that the maximum stresses are about 2.2 times the stresses in the median plane and yielding may therefore be expected when $\sigma = 1/2.2\ \sigma_{y.p.} = 0.45\ \sigma_{y.p.}$. These values agree quite well with general test experience, which indicates that slight set may be expected at about 0.5 $\sigma_{y.p.}$ and definite set at 0.7 $\sigma_{y.p.}$. Reference 3 gives the somewhat higher value 0.8 $\sigma_{y.p.}$; this difference may be caused by using panels with low values of h/t having considerable gusset effect or by allowing larger permanent deflections. As the permanent set of shear webs is frequently determined by visual inspection rather than by quantitative measurements, it is indeed surprising that different investigators agree so closely.

The high stresses just discussed are localized in the outside fibers of the sheet along the crests of the waves. When the stresses pass the yield point, ample opportunity is present for redistribution and equalization of stress; Wagner argued in reference 1 that this localized yielding would merely serve to hasten the attainment of a uniform diagonal-tension field. The ultimate strength of the web would then be reached when the stress in the median plane of the web $\sigma = 2\tau/C_2$ equals the ultimate allowable stress in tension.

According to the results of reference 7, this method of finding the ultimate strength of the web would apply even for a loading ratio below 2, that is, when the sheet has barely buckled. Consideration of the limiting case when the loading ratio is just above unity indicates that this method is probably too severe. If such a sheet is considered as a shear-resistant web, its strength will be found by comparing the shear stress τ with the ultimate shear stress τ_{ult}. If the same sheet is considered as an incomplete diagonal-tension field, its strength will be found by comparing $\sigma = 2\tau$ with σ_{ult}. The value of σ_{ult} being less than $2\tau_{ult}$, the second method of design would impose a weight penalty on the designer. Such a penalty seems unjustified because test experience indicates that the buckling of a flat sheet is a fairly gradual process so that no sudden change in design characteristics seems to be called for at the buckling point. It is therefore suggested that

the diagonal-tension stress be computed as $\sigma=2\tau/C_2$ in all cases and that the allowable ultimate stress be taken as

$$\sigma_{all}=2\tau_{ult}-k(2\tau_{ult}-\sigma_{ult}) \quad (22)$$

where k is the diagonal-tension fraction. When the web is in pure diagonal tension ($k=1$), then $\sigma_{all}=\sigma_{ult}$. When the web is in pure shear ($k=0$), then $\sigma_{all}=2\tau_{ult}$, or $\tau_{all}=\tau_{ult}$.

Allowance must be made for the weakening of the web by the rivet holes along the flanges and the unrights. This allowance may be made by multiplying the sheet thickness by the factor $(1-nd)$, where d is the diameter of a rivet and n is the number of rivets (in one row) per inch run along the flange or the upright. This correction is important because the rivet spacing along the flanges is often quite close.

A point that may cause some confusion should be mentioned here. It is fairly common engineering practice to test a series of diagonal-tension beams and to plot the results as allowable shear stresses. In most cases, the allowable shear stresses thus determined will not agree with those found by using formula (22). The test failures, however, are usually failures of the uprights; rupture of the web is comparatively rare. The test results should therefore be considered as giving not failing stresses of the webs but failing loads of the beams. These failing loads depend on all the properties of the beams; to plot them as a function of a single property is defensible merely as a measure of convenience and permissible only with the strict understanding that the results shall be applied exclusively to closely similar beams, unless there is definite evidence that the neglected properties play only an insignificant part. Unfortunately, the final curves of a test report commonly become separated from the report itself, making impossible the application of the results in the proper manner, namely, to beams similar to those originally tested.

ANALYSIS OF UPRIGHTS

Computation of stresses in the uprights.—The maximum stresses in uprights symmetrically arranged on both sides of the web occur at midheight and can be found by using either equation (13) or the design chart of figure 4. For values of h/t below 600, the computed stresses must be multiplied by a reduction factor k_σ taken from figure 14 with $y/t=h/2t$.

When the value of h/t is about 1,000 or higher, the computed stresses σ_U may be considered as group-average stresses for groups of three or more uprights working under identical conditions. Any individual upright of the group may have stresses 20 to 30 percent higher than the group average.

As the value of h/t decreases, the computed stresses σ_U become more conservative. At $h/t=500$ this conservatism is just about sufficient to offset variations from the group average, so that the computed stresses may be considered as maximum rather than as group-average stresses.

When the uprights are arranged on only one side of the web, the actual cross-sectional area of the uprights should be replaced by an effective area because the uprights will be not only in compression but also in eccentric bending, and the stress of the fibers adjacent to the web will be the sum of the compressive stress and the bending stress. By use of the elementary formulas for bending due to eccentric loading, the effective area of the uprights is found to be

$$A_e=\frac{A}{1+\left(\frac{e}{\rho}\right)^2} \quad (23)$$

where A is the actual area; e, the distance from the web to the centroid of the upright; and ρ, the centroidal radius of gyration of the upright for bending normal to the plane of the web. When this area A_e is used, the stress σ_U found from figure 4 will be the maximum stress in the upright and will occur in the fibers next to the web.

Allowance should be made for unintentional eccentricities that may exist even when the uprights are symmetrically arranged in pairs with respect to the web. In the N. A. C. A. tests, the eccentricities calculated from the individual strain readings sometimes reached the theoretical maximum, which is found by assuming that the bolt transferring the load from flange to upright bears only on one side of the web, that is, on one upright of the pair. In riveted connections, the average eccentricity will probably be smaller.

Determination of buckling stresses for uprights.—The available theory for determining allowable stresses or buckling stresses in uprights was discussed in part I. The main contribution of the theory is the establishment of an effective column length for bending failure. The actual column strength for any chosen section will probably quite often be determined by tests rather than by theoretical calculations. If these tests are made on uprights as free columns, careful consideration must be given to the possible effects of interaction between the uprights and the web.

The task of defining allowable stresses for uprights is extremely difficult. Aside from the fact that the theory is very incomplete, there also exists no unequivocal, generally accepted definition of the term "failure." Since the basic purpose of setting allowable stresses is the avoidance of failure, this lack of a definition is a severe handicap. Columns exhibit generally elastic instability of one type or another, and the onset of instability is termed "failure" in the theoretical text-books. The practical test engineer may observe this phenomenon but considered it merely as "slight waving"; in fact, in routine tests the phenomenon may go undetected because sensitive measurements may be necessary to discover it. From a practical point of

view, it is not so important to know the exact buckling load as it is to know how soon after passing the buckling load the deformations and the stresses become intolerably large. Unfortunately, this range is generally beyond the scope of the theory for complex structures.

The different meanings attributed to the word "failure" have created much confusion and uncertainty. It may be advisable to differentiate between impermissible failures, conditionally permissible failures, and permissible failures. Impermissible failures are, for instance, rupture of the web or shearing of the rivets between uprights and flanges. The best example of a permissible failure is a diagonal-tension web; such a web has failed by elastic instability under shear stresses.

Reference should be made to the tentative conclusions on strength of uprights in part II of this paper.

ANALYSIS OF RIVET CONNECTIONS

Rivets between web and flange.—If the web is working in shear, the running shear transmitted from the web to the flange is $q=S_w/h$ pounds per running inch. The force on each rivet is obtained by multiplying the running shear by the rivet pitch. If the web is in pure diagonal tension, the force transmitted is 1.414 S_w/h pounds per running inch, assuming the angle of diagonal tension to be 45°.

In an incomplete diagonal-tension field, the force transmitted between web and flange may be assumed to be between the two extremes given and proportional to the amount of diagonal tension, that is, equal to $(1+0.414\ k)\ S_w/h$, where k is the diagonal-tension fraction. This procedure is probably conservative when the web is clamped between two parts of the flange or when the web is stiffened by tensile stresses; under these conditions, the web in the vicinity of the rivets will be practically in pure shear. When the web is riveted to only one side of the flange, a similar effect will appear because the web is forced to remain more or less plane where it is in contact with the flange; on the other hand, the tendency of the web to form folds will put tensile forces on the rivets, so that greater margins of safety should be provided in such cases.

Web splices.—The design of web splices is, in principle, identical with the design of the joint between web and flange.

Rivets between uprights and web.—Theoretically, the uprights need not be riveted to the web; in two sets of the N. A. C. A. tests, the uprights were entirely free of the web. In practice, the uprights are probably always riveted to the web in order to take advantage of the bracing effect that the web exerts on the uprights. The strength of the uprights and the strength of the rivet connection are interdependent: one cannot be found unless the other is known. Obviously, then, any calculations would require the existence of a well-developed theory of the interaction between uprights and web. The discussion in part I showed the theory of interaction to be practically nonexistent; it is therefore impossible at present to design the rivet connection between uprights and web on a very rational basis. The only possible approach to the problem by theoretical means is to use the standard theory for shear in built-up structural columns; this theory may be found in many textbooks on structural engineering or strength of structures, for instance, in reference 12.

A minor criterion for a desirable rivet spacing can be established as follows for the case where the uprights are arranged on only one side of the web. In general, delaying the appearance of folds as long as possible will be desirable. To this end, the rivets attaching the uprights to the web should be spaced closely enough to give to the web the equivalent of a supported edge along the line of rivets. Test experience indicates that, in most cases, one diagonal-tension fold forms at each upright; that is, the wave length of the buckles is equal to the spacing of the uprights. In order to prevent this buckling at each upright, the rivet pitch should be less than or at most equal to one-fourth the wave length of the folds or the upright spacing, that is

$$p \leqq \frac{1}{4} d$$

If the rivet pitch is increased to equal the wave length or spacing, the folds can theoretically form across the uprights as though the uprights did not exist; the width of plate to be used in formula (16) for the critical shear stress will then be the depth of the beam instead of the spacing of the uprights and the critical shear stress will be very much reduced. Obviously, the fulfillment of this criterion for rivet pitch will be neither feasible nor necessary on shallow beams.

Rivets connecting uprights and flanges.—The end rivet or rivets connecting the uprights to the flanges carry the loads from the uprights into the flanges. These loads are obtained by finding the stresses in the uprights with the aid of figure 4 and multiplying the stresses by the areas of the uprights. The stresses in the uprights vary along the uprights in accordance with the gusset factor shown in figure 14; in order to find the load on the end rivets, the stress in the upright should be taken at the upright-to-web rivet nearest the flange.

An individual upright can evade general overstressing to some extent by buckling and throwing the load on the adjacent uprights. The end rivets cannot evade overstressing with any degree of effectiveness; they should therefore be considered the same as fittings, and the loads transmitted by the uprights should be multiplied by a factor of at least 1.2 to obtain the design loads on the rivets when the computed stresses in the uprights are group averages.

SHEAR STIFFNESS

In diagonal-tension beams, the shear deflections are of appreciable magnitude compared with the bending deflections and cannot be ignored, as in most other types of beam. A knowledge of the shear stiffness of diagonal-tension fields is, therefore, of some practical interest.

According to the basic assumption expressed by equation (7), there is a simultaneous action of shear force and diagonal-tension force. The total shear deformation is the sum of the deformations caused by these forces; the equivalent or effective shear modulus

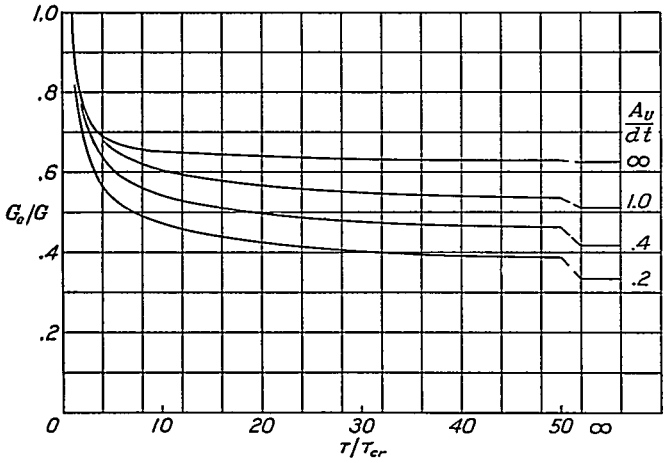

FIGURE 25.—Effective shear modulus (secant modulus) of incomplete diagonal-tension field.

G_e of the incomplete diagonal-tension field is therefore given by the equation

$$\frac{1}{G_e}=\frac{1-k}{G}+\frac{k}{G_{DT}} \tag{24}$$

where G is the shear modulus of the material of the sheet and G_{DT} is the effective shear modulus of the web when the web is working in pure diagonal tension.

According to reference 1, the effective shear modulus in pure diagonal tension is

$$G_{DT}=\frac{E}{4\sqrt{\left(1-\frac{\sigma_x}{\sigma}\right)\left(1-\frac{\sigma_y}{\sigma}\right)}} \tag{25}$$

In most practical cases, σ_x can be neglected in this expression because the flanges must be made heavy to carry the primary beam stresses. For $-\sigma_y$, the value σ_U is substituted because, in this paper, σ_U is understood to be a compression stress. Finally, by equation (3), $\sigma=2\tau$, assuming that C_2 can be taken as unity, and the formula for shear modulus becomes

$$G_{DT}=\frac{E}{4\sqrt{1+\frac{\sigma_U}{2\tau}}}$$

With the average value $E=2.5G$, this equation becomes

$$G_{DT}=\frac{0.625G}{\sqrt{1+\frac{\sigma_U}{2\tau}}} \tag{26}$$

With the help of equations (24) and (26) and the design chart of figure 4, curves of the ratio G_e/G have been computed for four values of A_U/td and for the same range of loading ratios τ/τ_{cr} as used in figure 4. These curves are plotted in figure 25. The shear stiffnesses given by these curves are somewhat lower than the corresponding values from reference 5; in the practical range of A_U/td, the difference is about 10 percent and varies but little with loading ratio up to loading ratios of 50. For the limiting cases of pure diagonal tension, the stiffnesses given by figure 25 agree with those of reference 5 within the accuracy of reading the curves.

LANGLEY MEMORIAL AERONAUTICAL LABORATORY,
NATIONAL ADVISORY COMMITTEE FOR AERONAUTICS,
LANGLEY FIELD, VA., *March 28, 1940.*

REFERENCES

1. Wagner, Herbert: Flat Sheet Metal Girders with Very Thin Metal Web. Pts. I, II, and III. T. M. Nos. 604, 605, and 606, N. A. C. A., 1931.
2. Kuhn, Paul: A Summary of Design Formulas for Beams Having Thin Webs in Diagonal Tension. T. N. No. 469, N. A. C. A., 1933.
3. Niles, Alfred S., and Newell, Joseph S.: Airplane Structures. Vol. I, 2d ed., John Wiley & Sons, Inc., 1938.
4. Timoshenko, S.: Theory of Elastic Stability. McGraw-Hill Book Co., Inc., 1936.
5. Lahde, R., and Wagner, H.: Tests for the Determination of the Stress Condition in Tension Fields. T. M. No. 809, N. A. C. A., 1936.
6. Schmieden, C.: Ebene Blechwandträger mit nicht-parallelen Holmen. Luftfahrtforschung, Bd. 13, Nr. 11, 20. Nov. 1936, S. 391–393.
7. Wagner, H., and Ballerstedt, W.: Tension Fields in Originally Curved, Thin Sheets during Shearing Stresses. T. M. No. 774, N. A. C. A., 1935.
8. Schapitz, E.: The Twisting of Thin-Walled, Stiffened Circular Cylinders. T. M. No. 878, N. A. C. A., 1938.
9. Schapitz, E.: Contributions to the Theory of Incomplete Tension Bay. T. M. No. 831, N. A. C. A., 1937.

10. Kuhn, Paul: Loads Imposed on Intermediate Frames of Stiffened Shells. T. N. No. 687, N. A. C. A., 1939.
11. Southwell, R. V., and Skan, Sylvia W.: On the Stability under Shearing Forces of a Flat Elastic Strip. Proc. Roy. Soc. (London), ser. A, vol. 105, no. 733, May 1924, pp. 582–607.
12. Timoshenko, S.: Strength of Materials. Pt. II. D. Van Nostrand Co., Inc., 1930.
13. Cox, H. L.: Summary of the Present State of Knowledge Regarding Sheet Metal Construction. R. & M. No. 1553, British A. R. C., 1933.
14. Seydel, Edgar: Wrinkling of Reinforced Plates Subjected to Shear Stresses. T. M. No. 602, N. A. C. A., 1931.
15. Seydel, Edgar: The Critical Shear Load of Rectangular Plates. T. M. No. 705, N. A. C. A., 1933.
16. Seydel, Edgar: Schubknickversuche mit Wellblechtafeln. Jahrb. 1931 der DVL, R. Oldenbourg (Munich), S. 233–245.
17. Schmieden, C.: Das Ausknicken versteifter Bleche unter Schubbeanspruchung. Z. F. M., 3.Heft, 21.Jahrg., 14. Feb. 1930, S. 61–65.
18. Lundquist, Eugene E., and Fligg, Claude M.: A Theory for Primary Failure of Straight Centrally Loaded Columns. T. R. No. 582, N. A. C. A., 1937.
19. Limpert, G.: Über die Knickung ebener Zugfeldträger. Jahrb. 1938 der deutschen Luftfahrtforschung, R. Oldenbourg (Munich), S. I427–I432.
20. Lundquist, Eugene E.: Local Instability of Centrally Loaded Columns of Channel Section and Z-Section. T. N. No. 722, N. A. C. A., 1939.
21. Anon.: Strength of Aircraft Elements. ANC–5, Army-Navy-Commerce Committee on Aircraft Requirements, U. S. Govt. Printing Office, Jan. 1938.

TABLE I

SCHEDULE OF N. A. C. A. STRAIN MEASUREMENTS

Type of upright	Web	Spacing of uprights		
		d=5 in.	d=10 in.	d=20 in.
Tests on 20-inch beam				
I	Clamped	20-1	20-2	20-3
II	do		20-4	20-5
Type I and II alternating	do		20-6	
Do	do		[a] 20-7	
Tests on 10-inch beam				
I	Clamped		10-1	
II	do	10-2	10-3	
I	Free	10-4	10-5	
II	do	10-6	10-7	

[a] For set-up 20-7, positions of type I and type II uprights were interchanged as compared with positions on set-up 20-6.

TABLE II

EFFECT OF DIAGONAL TENSION ON BUCKLING OF UPRIGHTS

[Basic data from reference 19; d/h=0.2; V_T/P_E=6.7; $P_E=\frac{\pi^2 EI}{h^2}$]

Specimen	σ_U/σ_E	k	$1+k^2D$	$\frac{\sigma_U}{\sigma_E(1+k^2D)}$
1	7.61	0.922	5.85	1.30
2	4.65	.872	3.34	.87
3	3.50	.670	3.56	1.01
4	3.13	.720	3.96	.79
Average				.99